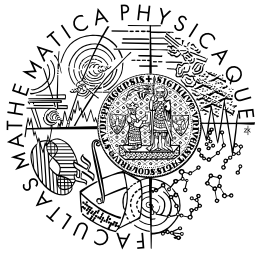

FACULTY
OF MATHEMATICS
AND PHYSICS
Charles University

MASTER THESIS

Vítek Veselý

Physics of extended objects in strong gravitational fields

Institute of Theoretical Physics

Supervisor of the master thesis: RNDr. Martin Žofka, Ph.D.
Study programme: Physics
Study branch: Theoretical Physics

Prague 2019

I declare that I carried out this master thesis independently, and only with the cited sources, literature and other professional sources.

I understand that my work relates to the rights and obligations under the Act No. 121/2000 Sb., the Copyright Act, as amended, in particular the fact that the Charles University has the right to conclude a license agreement on the use of this work as a school work pursuant to Section 60 subsection 1 of the Copyright Act.

In ..... date ..... signature of the author

I would like to thank my supervisor Martin Žofka for his useful and valuable advice, for his dedication in circumstances which would prevent many from finding time for our research and for his warm approach.

Title: Physics of extended objects in strong gravitational fields

Author: Vítek Veselý

Department: Institute of Theoretical Physics

Supervisor: RNDr. Martin Žofka, Ph.D., Institute of Theoretical Physics

Abstract: We study several different models of extended bodies in gravitational fields. Firstly, we revisit the glider model of a dumbbell-like oscillating body. We develop an independent scheme to integrate the equations of motion. We study the radial fall of a Newtonian spring, calculate the position shifts of the spring and find the critical value of the spring constant which cannot overcome the tidal forces. We argue that the relativistic glider model is unphysical due to its behaviour in the critical regions.
Secondly, we show that Dixon's theory of extended bodies predicts a geodesic motion of the centre of mass in maximally symmetric spacetimes. We prove that a system of test particles can be described by a conserved stress-energy tensor and we evaluate the position shifts of the glider model in the maximally symmetric spacetimes, showing its disagreement with Dixon's theory. We thus conclude again that the glider model must be rejected.
And thirdly, we study a model of an extended body consisting of interacting particles, which is in accord with Dixon's theory. We calculate the position shifts for this model and show that the model does not predict any measurable swimming effect. Finally, we estimate the numerical error of the calculation by finding the position shifts of the model in maximally symmetric spacetimes.

Keywords: general relativity, extended bodies, Dixon's formalism, relativistic glider.

Contents

Introduction

One of the oldest problems in physics is to predict the path of an object if we know its initial conditions and all the forces acting on it. In Newtonian mechanics, an object whose size is negligible and which is not influenced by any outer force moves at a constant velocity in a straight line. In fact, the centre of mass of any complex system behaves as a point particle moving in a force field which is the vector sum of all outer forces acting on all the individual parts of the body. Without any outer force or in case of a homogeneous force field, the centre of mass moves as if it were a single test particle with the total mass of the system.

In general relativity, a free test particle is an object of a negligible size whose motion is influenced only by gravity, which manifests itself as the curvature of spacetime. Such free test particles move along geodesics. However, because the individual parts of any finite body move in an external gravitational field, the centre of mass of a body whose size cannot be neglected does not behave as a single particle. In a general gravitational field, it is difficult to even define the centre of mass of a complex extended body because the notion of simultaneity of two distant events is not well-defined.

In the Newtonian case, the theory of extended bodies moving in gravitational fields has been of interest for the constructors of satellites in orbit because a controlled deformation of the object can alter its orbital parameters. The first paper discussing the tether-control of satellites appeared in the 1960s (see [1] for a review of literature) and the research continues to this day [2-4]. There have even been several in-orbit experiments (for example, the Gemini XI mission and, more recently, STARS-C aboard the ISS [5]).

In general relativity, there are two main effects resulting in a deviation from geodesic motion for an extended body: swinging and swimming. The swinging effect is present even in the Newtonian gravity. It describes how the body can gain energy in the gravitational field by expanding and contracting at appropriate moments just like a child on a swing gains energy by moving their body.

The swimming effect was first introduced by Jack Wisdom in [17]. The author argues that an extended body can change its position in a gravitational field because it is moving on a curved manifold. The object can achieve a net displacement simply by performing cyclical motion. The author also provides an example of a tripod swimming in the Schwarzschild spacetime. The swimming effect is purely relativistic in its nature. However, there have been papers which applied the same procedure as Wisdom to a tripod in the de Sitter universe [7] and obtained a similar result for the displacement. The authors argue that this result disproves Wisdom's original findings because it contradicts the predictions of a general theory of extended bodies presented by Dixon [8-10].

The predictions of general relativity for the motion of extended bodies can also be used to distinguish the characteristics of a given gravitational background which

would remain undetectable in a single-particle approach. For example, molecules oscillating near the ISCO orbit in an accretion disk near a black hole may be of interest [6].

In the Newtonian case, the controlled deformations of an extended body are often described by a controlled Lagrangian. The theory behind this approach has been studied since the 1990s, see, for example, [11-13]. Several papers have tried to apply a similar description to the problem of extended bodies undergoing controlled deformations in general relativity [14-16]. We studied the results of [14] in detail in the bachelor thesis [18] and published some of the results in [20]. The paper is attached as an appendix to the present thesis.

The aim of the present thesis is to study some of the proposed models of extended bodies in general relativity as well as their counterparts in the Newtonian theory and to further investigate these models. At the same time, we shall study some general predictions for the motion of a body described by a stress-energy tensor and we shall confront the studied models with these results.

The thesis is organised as follows: in Chapter 1, we study the model presented in [14] in further detail. We develop an independent scheme to calculate the net position shifts of the model, use the scheme to find the limits of the description and also study a simple energy-conserving model in the Newtonian gravitational field to better understand the behaviour of the model in the critical regions. Chapter 2 introduces the general theory of extended bodies as presented by Dixon and applies the theory to a system of free particles which interact only during collisions. Furthermore, we confront the predictions of the glider model from [14] with the results of Dixon's theory for objects moving in maximally symmetric spacetimes. In Chapter 3, we present a model of an extended body consisting of particles moving along geodesics, which undergo decays and collisions and compare the predictions of this model to the glider model of [14] and to the results of Dixon's theory.

1. Remarks on the relativistic glider

In the first chapter, we study the predictions of a simple relativistic model of an extended body called the relativistic glider. This model was introduced in a paper by E. Guéron and R. A. Mosna [14]. The authors propose a dumbbell-like, oscillating test object moving radially in the Schwarzschild spacetime.

We studied this model in [18], where we numerically solved the proposed equations of motion of the body to independently verify the results of [14] and to find the predictions of the model in the extreme cases of the relevant parameters where the relativistic effects become significant. This includes the region of very fast and very slow expansion rates of the body and the case of multiple oscillations. Furthermore, we showed how the maneuver affects the speed of the dumbbell.

The glider model is interesting because its predictions vary from the predictions of a similar model in the Newtonian gravitational field. Specifically, it predicts that the relativistic body can slow down its fall by performing an expansion and a contraction with a predetermined deformation function. This slowing down is present even at speeds which are much lower than the local value of the speed of light.

On the other hand, the Newtonian model predicts that the net displacement of the body is always negative, i.e., that the extended body falls faster than a reference point particle. Unlike its relativistic counterpart, the Newtonian effect vanishes for faster oscillations of the body, which allows us allow us to distinguish observationally between the two theories, perhaps providing information about the central gravitating object.

Apart from this, we also applied the model to the case of a body oscillating perpendicularly to the trajectory of its centre of mass. This case may be of interest to the constructors of satellites because the displacement effect is several orders of magnitude larger than in the case of the radial oscillations. However, the Newtonian swinging effect is the dominant effect in this case and, therefore, this model is not suitable for studying the relativistic effects.

Since its publication, there have been objections to the glider model of [14] and to the examples of the swimming effect proposed by Wisdom [7] because an analogous analysis predicts the appearance of the swimming effect in maximally symmetric spacetimes where no net displacement of any extended body is possible as we show in Chapter 2.

Our original goal was to expand the results of the model in the critical regions. In this chapter, we propose an independent scheme which expresses the displacement of the body as a correction to geodesic motion, significantly increasing the numerical credibility of the results because the net displacement is no longer ex-

pressed by subtracting two very close values.

We also study a simple spring model in the Newtonian gravitational field. The results are then used to interpret the predictions of the glider model and, ultimately, to show that the glider model is insufficient in the most interesting cases where the net displacement apparently diverges and the swinging effect could be observable.

1.1 Description of the model

The glider consists of two equal mass points which interact via a massless rod, whose length can be modified by an engine. The body falls radially in the Schwarzschild spacetime with mass M. We shall use the coordinate time t as the independent variable parametrization of the motion. For further discussion about the choice of the independent variable see [18]. We shall use the following Lagrangian to derive the equations of motion:

$$\begin{aligned} L_d = &- m\sqrt{\left(1-\frac{2M}{r_d}\right)-\frac{1}{1-\frac{2M}{r_d}}\left(\frac{\mathrm{d}r_d}{\mathrm{d}t}\right)^2} \\ &- m\sqrt{\left(1-\frac{2M}{r_d+l}\right)-\frac{1}{1-\frac{2M}{r_d+l}}\left(\frac{\mathrm{d}r_d}{\mathrm{d}t}+\frac{\mathrm{d}l}{\mathrm{d}t}\right)^2}, \end{aligned} \tag{1.1}$$

where r_d is the coordinate position of the lower point of the glider and l is the coordinate length of the body. We must realise, that in this case $l(t)$ does not represent a degree of freedom of the system but a fixed function of time. The engine inside the glider ensures that the prescribed coordinate distance is maintained throughout the maneuver. This description falls under the category of the so-called controlled Lagrangians.

Although the theory of controlled Lagrangians is mostly accepted in the Newtonian description, it can be a source of unphysical effects in relativistic theories because it requires the non-causal behaviour of the bond. The prescribed deformation function $l(t)$ represents a coordinate distance on a given spacelike hypersurface of constant t, but there is no causal way either of the endpoints of the body could know the position of the other on that hypersurface.

Moreover, the description cannot even realistically account for any transfer of energy between the masses because it lacks any kinetic term for the bond. Despite all this we shall accept this model in this chapter to study its predictions in both the weak-field, slow-motion regime where its Newtonian limit should be physical, and in the highly relativistic case. Eventually, we shall show several more of its problems.

Our main goal is to study the effect of non-locality of the body on its motion. Specifically, we shall compare the motion of the dumbbell with the motion of a test

point particle with the same initial conditions and described by the Lagrangian:

$$L_p = -m\sqrt{\left(1-\frac{2M}{r_p}\right) - \frac{1}{1-\dfrac{2M}{r_p}}\left(\frac{\mathrm{d}r_p}{\mathrm{d}t}\right)^2}. \tag{1.2}$$

The principle of stationary action with this Lagrangian leads to the radial geodesic equation for the Schawrzschild metric as we show in Chapter 3. To quantify the deviation from the geodesic motion we use the quantity δr, which we shall call position shift. It is defined by:

$$\delta r = r_d + \frac{l}{2} - r_p. \tag{1.3}$$

Another relevant variable is the velocity shift $\delta\dot{r}$, sometimes referred to as differential velocity:

$$\delta\dot{r} = \dot{r}_d + \frac{\dot{l}}{2} - \dot{r}_p. \tag{1.4}$$

The dot represents a derivative with respect to t. Both of these functions are defined in terms of coordinates, they are therefore non-covariant. However, both of the relevant coordinates r and t have a well-understood physical interpretation for a stationary observer at radial infinity. The position shift describes the difference of position of the dumbbell and that of the point mass whenever the endpoints of the dumbbell coincide. If the dumbbell is expanded, the position shift represents the coordinate position of the geometric centre of the dumbbell relative to the point mass.

The results depend on the choice of the deformation function. The authors of the original paper [14] used:

$$l(\alpha,\omega t) = \delta l\ \exp\left[\frac{(1+\alpha-2\omega t)^2}{(1+\alpha^2)\omega t(-1+\omega t)}\right], \tag{1.5}$$

where δl is the maximal length of the dumbbell, α is an asymmetry parameter of the function and ω is another parameter, which is related to the periodicity and rate of expansion of the dumbbell because the deformation function vanishes for $\omega t = 1$. This function, however, is not very suitable for numerical computations since it is not analytic at the endpoints of motion where the dumbbell shrinks to a point. Therefore, we used this form of the deformation function:

$$l(\alpha,\omega t) = \frac{\delta l}{2}(1-\cos\left[2\pi\omega t\{\alpha(\omega t-1)+1\}\right]) \tag{1.6}$$

with similar interpretations of the parameters. Further discussion about the choice of the deformation function can be found in [18] but an important property of both of them is that the value of the function as well as the first derivative vanishes for $t = 0$ and $t = 1/\omega$. We shall sometimes refer to ω as "frequency" even though we usually consider only one expansion-contraction stroke of the dumbbell, not any kind of periodic motion.

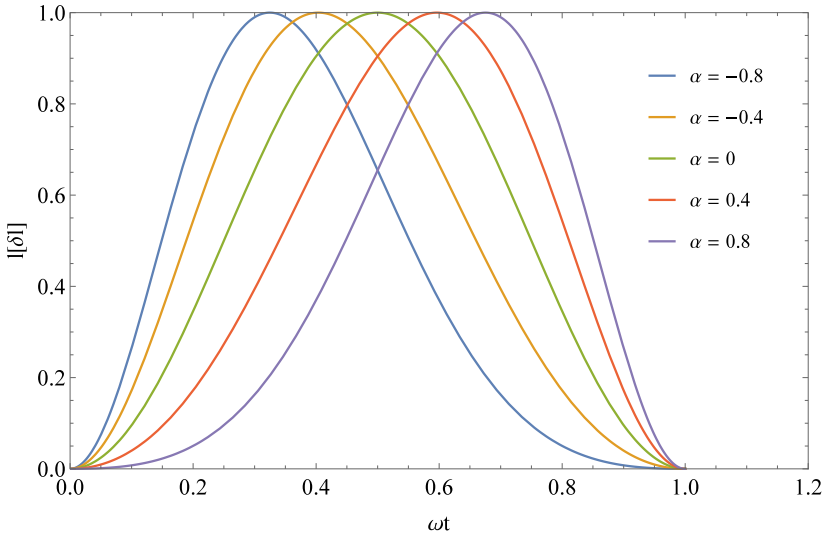

Figure 1.1: The selected shape of the deformation function of the dumbbell for five different values of the asymmetry parameter α. The dumbbell shrinks back to a single point after the time $1/\omega$ and the rate of its expansion also vanishes there. For negative α, the dumbbell expands rapidly and then shrinks back slowly. The opposite is true for positive α.

The goal is to solve numerically the equations of motion for the dumbbell for $t \in [0, 1/\omega]$ for different values of α and then evaluate the position shift and the velocity shift at the end of the integration. The original paper explored the positions shifts for ω's ranging from about $0.001M^{-1}$ to $0.07M^{-1}$. For frequencies above $0.02M^{-1}$ the position shifts reached a plateau which the authors described with the following semi-empirical formula:

$$\delta r \approx \Gamma(\alpha)\frac{\delta l^2}{R_0^2}M, \tag{1.7}$$

with $\Gamma(\alpha)$ being a dimensionless function of the asymmetry parameter. The body is dropped from $r = R_0$ with a vanishing initial velocity. In particular, the numerical values of the relevant length scales are: $R_0 = 120M$, $\delta l = 5 \times 10^{-3}M$. We shall explore this model in further detail and focus on some interesting parts of the plots of the shifts.

1.2 Alternative method of computation of the shifts

Let us first address the issue of the validity of the results obtained by direct numerical evaluation. In [18], we have already expressed our concerns about the fact that the final presented values of the position and velocity shifts are expressed as a result of subtraction of the positions of the free-falling body and the glider, which are very close. It is therefore reasonable to question the numerical error of these values. To this end, we integrated the equations of motion using several different numerical methods as well as two different mathematical software programmes (Wolfram Mathematica and Maple). We then concluded that the numerical error

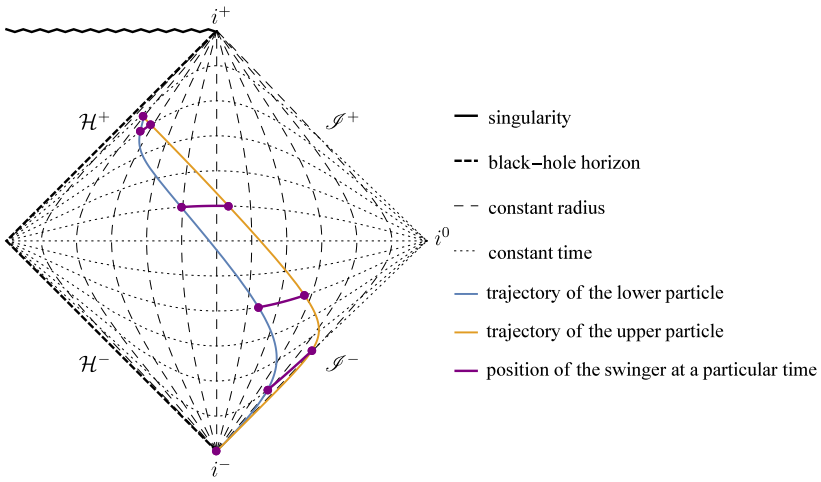

Figure 1.2: This figure depicts the evolution of the dumbbell in the Penrose diagram. The initial conditions and parameters were chosen rather extreme to make the diagram more legible. In this motion, $\omega = \frac{1}{107}M^{-1}$, the maximal length is $\delta l = 8M$ and the initial position $r_d(0) = 19M$. Neither of the two endpoints of the dumbbell can cross the event horizon in finite coordinate time because the horizon coincides with $t \to \infty$.

from the computation is orders of magnitude lower than the relevant position and velocity shifts and thus, that the presented results are a genuine feature of the solutions of the equations of motion.

However, it is still desirable to find a method which would not rely on the subtraction of the two close values. In this section, we present an alternative method which will allow us to compute the sought values using an expansion of the solution into an infinite series. We shall begin by creating a general framework which will allow us to compute the position shift of the dumbbell as a deviation from the geodesic motion.

We consider an action dependent on a small dimensionless parameter ϵ.

$$S = \int L(q, \dot{q}, t; \epsilon)\mathrm{d}t \tag{1.8}$$

Here, t is the independent variable, q represents the dependent function of t which should extremize the action. We consider only a 1-dimensional problem but this framework can be easily generalized to multidimensional problems. Dot represents a total derivative with respect to the independent variable t. The full equation of motion for $q = q(t)$ is:

$$\frac{\delta L}{\delta q} = \frac{\mathrm{d}}{\mathrm{d}t}\left(\frac{\partial L}{\partial \dot{q}}\right) - \frac{\partial L}{\partial q} = \frac{\partial^2 L}{\partial \dot{q}^2}\ddot{q} + \frac{\partial^2 L}{\partial q \partial \dot{q}}\dot{q} + \frac{\partial^2 L}{\partial t \partial \dot{q}} - \frac{\partial L}{\partial q} = 0. \tag{1.9}$$

We assume that we can express the solution of 1.9 as an infinite series:

$$q(t) = \sum_{n=0}^{\infty} q_n(t)\epsilon^n. \tag{1.10}$$

We can plug this Ansatz into 1.9 and since we want to satisfy this equation for an arbitrarily small value of ϵ, we can expand the left-hand side of the equation into an infinite series in ϵ as well.

$$\sum_{n=0}^{\infty} E_n(q_i, \dot{q}_i, t)\epsilon^n = 0 \tag{1.11}$$

The terms $E_n(q_i, \dot{q}_i, t)$ in the expansion do not depend on ϵ. The zeroth-order term in the expansion is:

$$E_0 = \frac{\partial^2 L}{\partial x_2^2}\ddot{q}_0 + \frac{\partial^2 L}{\partial x_1 \partial x_2}\dot{q}_0 + \frac{\partial^2 L}{\partial t \partial x_2} - \frac{\partial L}{\partial x_1}. \tag{1.12}$$

For clarity, we changed the notation of the partial derivatives of the Lagrangian with respect to the dependent variable. The partial derivative with respect to x_1 represents the derivative with respect to q and x_2 is the derivative with respect to $\dot{q}$. All the derivatives of the Lagrangian are evaluated at $(x_1, x_2, t; \epsilon) = (q_0, \dot{q}_0, t; 0)$.

We can see that the zeroth term of the expansion is identical to the left-hand side of the equation of motion for the original Lagrangian with $\epsilon = 0$. Similarly, we can express the first-order term:

$$\begin{aligned} E_1 = &\frac{\partial^3 L}{\partial x_1 \partial x_2^2}\ddot{q}_0 q_1 + \frac{\partial^3 L}{\partial x_2^3}\ddot{q}_0 \dot{q}_1 + \frac{\partial^3 L}{\partial \epsilon \partial x_2^2}\ddot{q}_0 + \frac{\partial^2 L}{\partial x_2^2}\ddot{q}_1 \\ +&\frac{\partial^3 L}{\partial x_1^2 \partial x_2}\dot{q}_0 q_1 + \frac{\partial^3 L}{\partial x_1 \partial x_2^2}\dot{q}_0 \dot{q}_1 + \frac{\partial^3 L}{\partial \epsilon \partial x_1 \partial x_2}\dot{q}_0 + \frac{\partial^3 L}{\partial x_1 \partial t \partial x_2}q_1 + \\ &+\frac{\partial^3 L}{\partial t \partial x_2^2}\dot{q}_1 + \frac{\partial^3 L}{\partial \epsilon \partial t \partial x_2} - \frac{\partial^2 L}{\partial x_1^2}q_1 - \frac{\partial^2 L}{\partial \epsilon \partial x_1} \end{aligned} \tag{1.13}$$

and so on. Since the right-hand side of the original equation of motion does not depend on ϵ, each term E_n in the expansion of the left-hand side must be equal to 0 for any t. We thus get an infinite set of equations $E_n = 0$ for the functions $q_i = q_i(t)$. These equations are coupled. However, the k-th equation depends only on q_i for $i \leq k$. We can thus solve the zeroth-order equation for $q_0(t)$, then plug this solution into E_1, solve for $q_1(t)$ and continue in this manner with the next terms. Let us assume for simplicity that the initial conditions for $q = q(t)$ are independent of ϵ, such as $q(t = 0) = r_0$, $\dot{q}(t = 0) = v_0$. Then the initial conditions for the functions $q_i(t)$ are: $q_0(t = 0) = r_0$, $\dot{q}_0(t = 0) = v_0$ and $q_i(t = 0) = 0$, $\dot{q}_i(t = 0) = 0$ for $i > 0$. If the initial conditions do depend on ϵ, one can expand the initial conditions into an infinite series and find the initial conditions for all the functions $q_i(t)$. We can also notice the structure of the partial equations of motion $E_k = 0$. Except for $k = 0$, the k-th equation of motion is an inhomogeneous linear differential equation for $q_k(t)$ and we have thus effectively linearized the equations of motion.

We could also ask whether it is possible to obtain the partial equations of motion directly from the original Lagrangian if we plug in the expansion of the solution.

$$L(q, \dot{q}, t; \epsilon) = L(\sum_{n=0}^{\infty} q_n(t)\epsilon^n, \sum_{n=0}^{\infty} \dot{q}_n(t)\epsilon^n, t; \epsilon) \tag{1.14}$$

We can now expand the Lagrangian into an infinite series of partial Lagrangians:

$$L(\sum_{n=0}^{\infty} q_n(t)\epsilon^n, \sum_{n=0}^{\infty} \dot{q}_n(t)\epsilon^n, t; \epsilon) = \sum_{n=0}^{\infty} L_n(t)(q_i, \dot{q}_i, t)\epsilon^n. \tag{1.15}$$

The first three terms in the expansion are:

$$L_0 = L(q_0, \dot{q}_0, t; 0), \tag{1.16}$$

$$L_1 = \frac{\partial L}{\partial x_1} q_1 + \frac{\partial L}{\partial x_2}\dot{q}_1 + \frac{\partial L}{\partial \epsilon}, \tag{1.17}$$

$$\begin{aligned} L_2 =& \frac{1}{2}\frac{\partial^2 L}{\partial x_1^2} q_1^2 + \frac{\partial^2 L}{\partial x_1 \partial x_2} q_1 \dot{q}_1 + \frac{\partial^2 L}{\partial \epsilon \partial x_1} q_1 + \frac{1}{2}\frac{\partial^2 L}{\partial x_2^2}\dot{q}_1^2 + \\ &+ \frac{1}{2}\frac{\partial^2 L}{\partial \epsilon^2} + \frac{\partial^2 L}{\partial \epsilon \partial x_2}\dot{q}_1 + \frac{\partial L}{\partial x_1} q_2 + \frac{\partial L}{\partial x_2}\dot{q}_2. \end{aligned} \tag{1.18}$$

Once again, all the partial derivatives of the Lagrangian are evaluated at the point $(x_1, x_2, t; \epsilon) = (q_0, \dot{q}_0, t; 0)$ and the k-th partial Lagrangian L_k depends only on $q_i(t)$ and its derivatives for $i \leq k$. If we try to find the equation of motion for $q_0(t)$ as:

$$\frac{\delta L_0}{\delta q_0} = \frac{\mathrm{d}}{\mathrm{d}t}\left(\frac{\partial L_0}{\partial \dot{q}_0}\right) - \frac{\partial L_0}{\partial q_0} = 0, \tag{1.19}$$

we find out that we obtain the same equation as from the expansion of the original equation of motion, i.e., $E_0 = 0$. Similarly, we could expect to find the k-th equation of motion as:

$$\frac{\delta L_k}{\delta q_k} = 0. \tag{1.20}$$

Unfortunately, this approach is wrong because even for the first equation we only obtain:

$$\frac{\delta L_1}{\delta q_1} = E_0. \tag{1.21}$$

The correct way to find the first partial equation is to differentiate L_1 with respect to q_0.

$$E_1 = \frac{\delta L_1}{\delta q_0} \tag{1.22}$$

Similarly, we can verify that we obtain the first three partial equations of motion after a longer but straightforward computation from the second partial Lagrangian L_2 as:

$$\begin{aligned} E_0 &= \frac{\delta L_2}{\delta q_2}, \\ E_1 &= \frac{\delta L_2}{\delta q_1}, \\ E_2 &= \frac{\delta L_2}{\delta q_0}. \end{aligned} \tag{1.23}$$

It seems reasonable to assume that, in general, we can obtain the left-hand side of the $(k-i)$-th partial equation of motion E_{k-i} by differentiating the k-th partial Lagrangian L_k with respect to the i-th function $q_i(t)$. However, we were not

able to prove this relation in the general case and so we shall apply this former expansion method in the rest of the present section.

We can now apply this procedure to the problem of a falling dumbbell described by the Lagrangian 1.9. We shall rewrite the deformation function as $l(t) = \delta l \cdot \lambda(t)$. Now, we can expand the solution in terms of δl or more precisely $\delta l/M$, which would be our ϵ as per above. The new variable $\lambda(t)$ is now of a similar order as $r_d(t)/M$.

We can expand the sought solution according to our scheme. We shall only use the first three terms of the expansion:

$$r_d(t) = r_0(t) + r_1(t)\frac{\delta l}{M} + r_2(t)\left(\frac{\delta l}{M}\right)^2. \tag{1.24}$$

If we now evaluate the relevant equations of motion according to our scheme, we find out that the zeroth equation of motion is twice the geodesic equation for a free-falling point expressed from 1.2. This is no surprise because we already know that the zeroth equation corresponds to the equation of motion for the original Lagrangian with the expansion parameter set to 0. In our case, if we set $\delta l = 0$, we are left with twice the Lagrangian for a free-falling particle. This confirms that in the lowest order of the expansion, the dumbbell falls as a free point particle along a geodesic.

The equation for the first correction is much more complicated. Furthermore, it is only possible to express the solution of the radial geodesic for the Schwarzschild spacetime as a parametric solution or as an inverse function $t = f(r_0)$, where f is expressed in terms of an integral. Fortunately, we can guess the solution of the equation for the first correction. If we set:

$$r_1(t) = -\frac{\lambda(t)}{2}M, \tag{1.25}$$

the equation for the first correction is satisfied identically. This solution also vanishes at the beginning as required by the initial conditions and is therefore our desired correction. Since our deformation function $\lambda(t)$ vanishes for $\omega t = 1$ for any value of the parameter α, the first correction does not contribute to the position shift of the dumbbell.

In a similar way, we can evaluate the equation of motion for the second correction. In the end, we are only interested in the numerical values of the position shifts. We don't need to worry about the problems with expressing the solution of the radial geodesic equation. We can simply use the numerical solution for our equation. We can and will, however, use the exact solution for $r_1(t)$. If we numerically integrate the equation of motion for the second correction, we obtain a non-vanishing value for $r_2(t)$ at $\omega t = 1$. This value after multiplying by $\delta l/M$ corresponds to the lowest non-vanishing order of correction. This fact explains the dependence on δl in the semi-empirical formula 1.7.

The computed values of the position shift correspond very well with the results

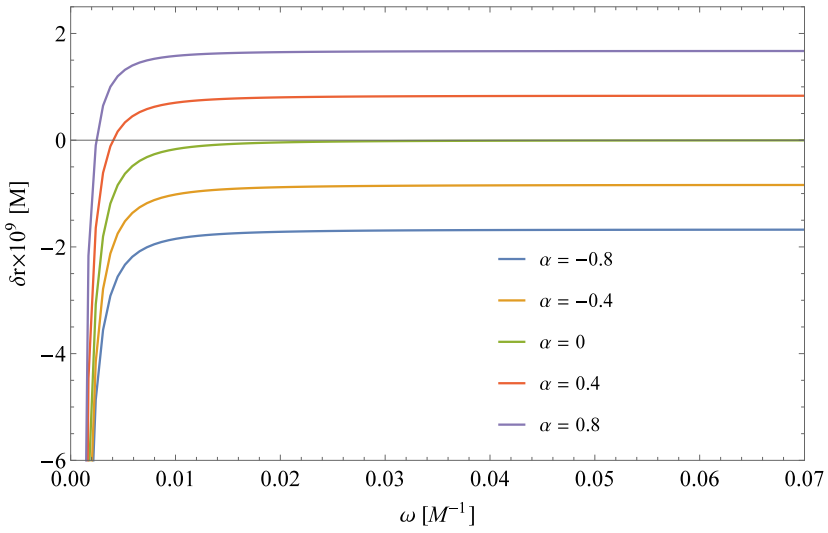

Figure 1.3: Position shifts of the dumbbell in the relativistic case calculated by an alternative approach using a Taylor expansion of the equations of motion. The results coincide very well with the values calculated by directly integrating the full equations of motion and subtracting the position of the free-falling point particle. The obtained shift is a result of the second-order correction to the geodesic motion in the expansion in δl.

from the direct integration, which confirms that the results are not distorted by a numerical error in a significant way. The main benefit of the expansion approach is its high speed of integration compared to the numerical solution of the original equation of motion. Additionally, it is much more robust numerically, enabling us to find the solution for a broader range of the parameters.

We also tried to use this approach to find an analytic expression for the function $\Gamma(\alpha)$ in 1.7. For high frequencies, the free-falling particle doesn't have enough time to start falling very fast, so we tried to approximate the geodesic motion with a constant $r_0(t) = R_0$. Unfortunately, the correction r_2 vanishes with this approximation. After using higher-order corrections for the geodesic motion, we were able to reconstruct the positions shifts but the equations of motion were too complex for us to find any analytic expression for the function $\Gamma(\alpha)$.

We also applied this procedure to the Newtonian case and once again, the zeroth-order solution corresponds to the problem of a free-falling particle in the central Newtonian gravitational field, the first-order correction is the symmetric motion of the endpoints of the dumbbell around the reference point and the second-order correction is the lowest non-vanishing contribution to the position shift and differential velocity.

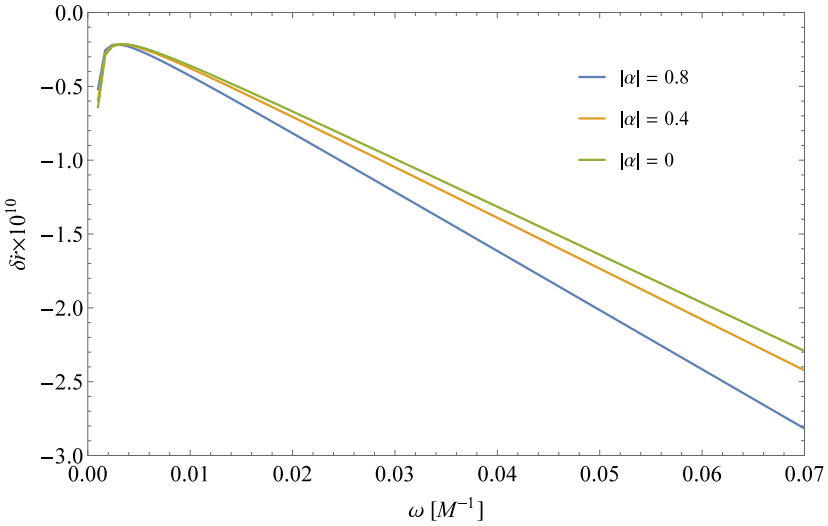

Figure 1.4: Velocity shifts of the dumbbell in the relativistic case calculated by an alternative approach using a Taylor expansion of the equations of motion. Once again, one can clearly see that $\delta\dot{r}$ does not vanish for the larger values of the parameter ω and it is almost independent of the sign of α. Again, the results coincide with the data obtained from direct integration of the equation of motion, confirming thus that the values are not heavily distorted by a numerical error.

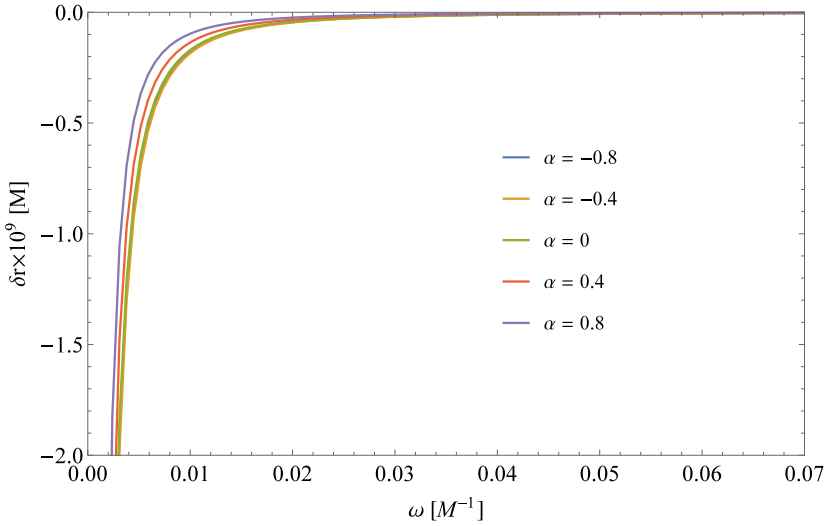

Figure 1.5: Position shifts of the dumbbell in the Newtonian case calculated by an alternative approach using a Taylor expansion of the equations of motion. Also in this case, the shifts come from the second-order correction to the motion of the free-falling body.

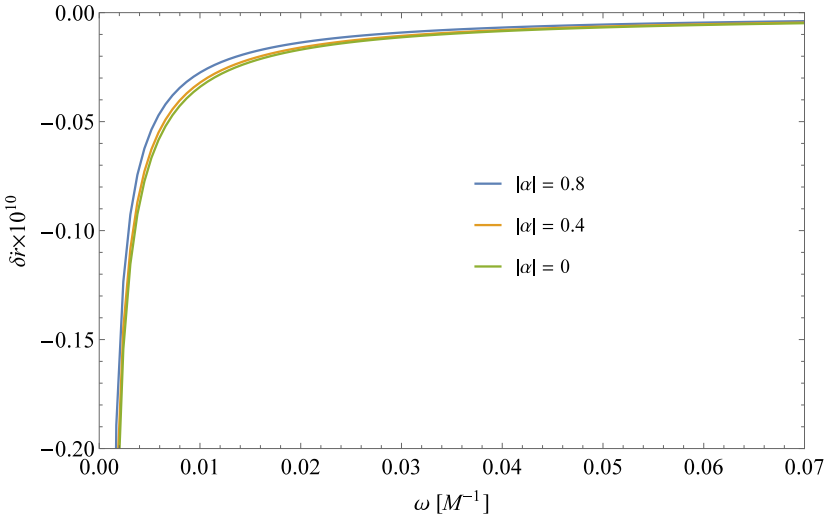

Figure 1.6: Velocity shifts of the dumbbell in the Newtonian case calculated by an alternative approach using a Taylor expansion of the equations of motion. Similarly to the relativistic case, the differential velocity is always negative indicating a greater velocity of the dumbbell towards the gravitational centre.

1.3 Computation of the critical values of the parameter ω and the behaviour of the model near the critical regions

After establishing the validity of the results of the numerical integration of the equations of motion, we can now proceed with further analysis of the model of the dumbbell-like body. In particular, we are most interested in the behaviour of the model in the limiting regions of the possible values of the parameter ω. The authors of the original paper [14] showed the apparent divergence of the position shifts δr in the region of small values of ω without further discussing its significance.

This rapid decrease of the position shift cannot, however, be a true divergence in the sense that there exists a limiting value of the parameter for which the absolute value of the position shift becomes larger than any scale for a very simple reason. The position shift is calculated as a result of two finite values of the coordinate positions of the two test objects. Since the position shift is negative, the dumbbell is even lower than the point mass which starts from rest at $R_0 = 120M$ and falls towards the gravitational centre. This means that the position shift is clearly bounded from below. Nevertheless, we shall still refer to this behaviour as "divergence".

Similarly, the differential coordinate velocity $\delta\dot{r}$ is bounded for both objects by the local value of the coordinate speed of light. This, of course, is not true for the Newtonian case. The position shift divergence is present in both the relativistic and Newtonian cases. In the latter, we speculated that the behaviour is linked to the existence of a critical value of the parameter ω where the physics changes. In particular, after a time $t = 1/\omega$ the point particle reaches the gravitational

centre where the acting force diverges. This means that the model clearly has to become invalid at this point, if not sooner. On the other hand, the relativistic objects are slowed near the event horizon of the black hole, which they cannot cross in finite coordinate time due to the nature of the coordinate system. Furthermore, we noticed that the divergence in the differential velocity also happens in both theories although it appears for much lower values of the parameter ω in the relativistic case.

The authors of [14] also mention possible problems with causality for large values of ω but they never discuss the critical values or the behaviour of the relevant variables in this region. In [18], we already tried to compute the critical values of ω by approximating the spacetime as flat and using the critical frequencies from the Minkowski spacetime. We concluded that in the relativistic case the position shifts stay almost constant up to the critical values of ω for each α at which point the equations of motion become singular and we are not able to continue with the integration.

We found this conclusion to be false by further inspection of this region. First of all, the expansion of the solution from the previous section allowed us to compute the critical values much more precisely. The equations of motion become singular if either of the parts of the dumbbell reaches the speed of light. Above the event horizon, this condition translates to:

$$\left|\frac{\mathrm{d}r}{\mathrm{d}t}\right| = 1 - \frac{2M}{r}, \tag{1.26}$$

where r is the position of either end of the dumbbell. We shall use the first-order correction from the expansion of the solution for $r = r(t)$, i.e., $r(t) = r_p(t) \pm \delta l \cdot \lambda(t)/2$. We make one more approximation to calculate the critical values. For the largest values of the parameter ω the free-falling particle does not have enough time to start moving before the time $t = 1/\omega$ and thus, we can assume that $r_p(t) \approx R_0$. Finally, λ is a function of both t and ω. However, it depends only on the product of these two variables, $\lambda(t, \omega) = \lambda(t\omega) \equiv \lambda(x)$ with $x \in [0, 1]$. The critical causality condition then reads:

$$\frac{\omega \cdot \delta l}{2}\left|\frac{\mathrm{d}\lambda}{\mathrm{d}x}\right| = 1 - \frac{2M}{R_0 \pm \delta l \cdot \lambda(x)}. \tag{1.27}$$

This equation has the form $\omega g(x) = h(x)$. We can safely divide the equation by $g(x)$ since $g(x) = 0$ indicates the slowest expansion rate of the dumbbell, not the fastest. We are looking for the smallest value of ω which satisfies this equation. We can therefore differentiate the equation with respect to x and find the extremal value by setting the derivative equal to 0. This leads to the equation:

$$g'(x)h(x) = g(x)h'(x). \tag{1.28}$$

This equation can be solved numerically for x for any value of α, R_0 and δl. We typically find two roots for each endpoint of the dumbbell and thus 4 roots in total. We then compute ω for each of these roots and the critical value is the smallest of these values.

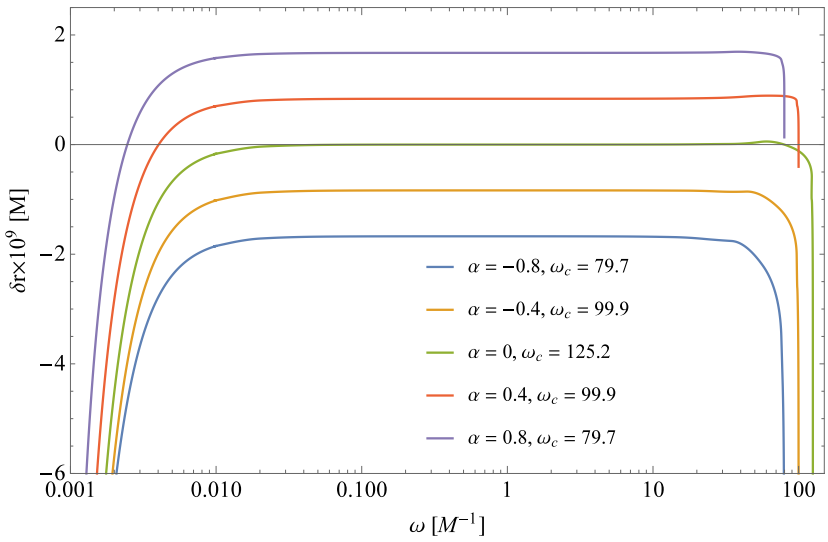

Figure 1.7: Position shifts in the relativistic case in the whole set of accessible values of the parameter ω. One can observe an apparent divergence in the regions of large and small values of ω. The position shift is positive for positive values of the asymmetry parameter α on the plateau. The values of the parameter ω_c are estimates of the critical frequencies at which one of the endpoints of the dumbbell exceeds the speed of light.

This approach offers a more precise estimation of the critical values of the parameter ω. We were then able to carefully approach these values while integrating the equations of motion of the dumbbell and we discovered a second divergence of the position shifts in the relativistic case near these critical values.

To conclude, we ultimately computed the position shifts for all possible values of the parameter ω. The results are shown in Figures 1.3, 1.8, 1.9 and 1.10. The Newtonian model predicts only the low-frequency divergence and the position shifts are always negative whereas the relativistic model predicts positive displacement, i.e., slower fall of the glider. This result seems to indicate the presence of the swimming effect.

1.4 Radial fall of a Newtonian spring in a central gravitational field

In this section, we shall study a simple model of a classical body falling radially in a central gravitational field. The body consists of two equal masses m connected by a massless spring with a spring constant $k \cdot m$. We chose this rescaling because we want to divide the Lagrangian by the mass m. This means that after the division the Lagrangian is independent of the mass of the endpoints. We denote the rest length of the spring l_0. The system is described by a classical Lagrangian:

$$L_s = \frac{1}{2}\left(\frac{\mathrm{d}r_1}{\mathrm{d}t}\right)^2 + \frac{1}{2}\left(\frac{\mathrm{d}r_2}{\mathrm{d}t}\right)^2 + \frac{M}{r_1} + \frac{M}{r_2} - \frac{1}{2}k(r_2 - r_1 - l_0)^2. \tag{1.29}$$

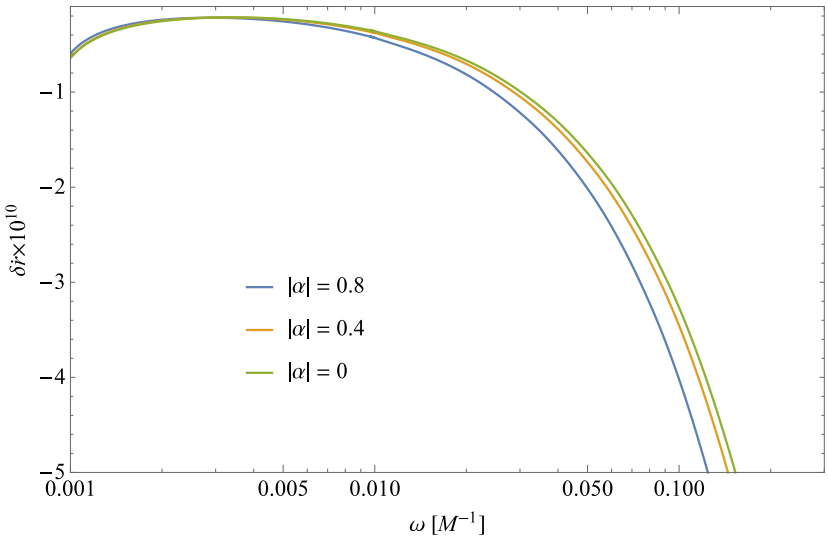

Figure 1.8: Differential velocity in the relativistic case. The apparent divergence for the slow expansion of the dumbbell begins at a smaller value of the parameter ω in comparison with the position shifts. The shift is always negative, which indicates a greater velocity towards the gravitational centre, almost independent of the sign of α and decreases more rapidly for the larger values of ω.

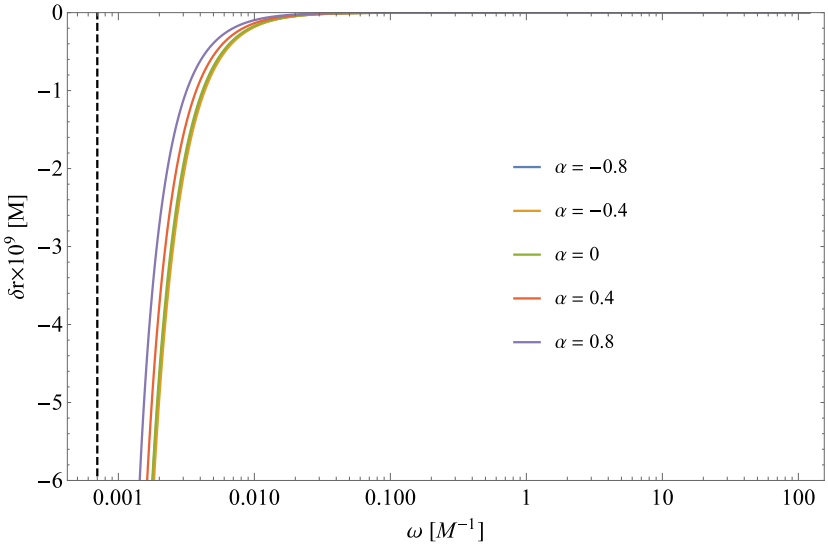

Figure 1.9: Position shifts in the Newtonian case. There isn't any apparent divergence for arbitrarily large values of the parameter ω. However, we can observe the apparent divergence in the region of small ω's. The dashed line represents a critical frequency $\omega_c \approx 6.8 \times 10^{-4}/M$ for which it would take a point mass falling from rest from $R_0 = 120M$ time $t = 1/\omega_c$ to reach the gravitational centre.

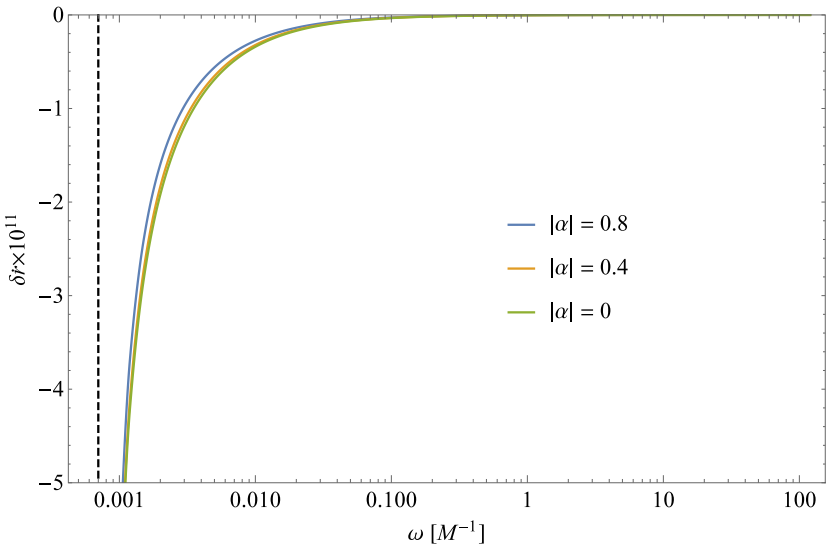

Figure 1.10: Differential velocities in the Newtonian case. The shifts are always negative and almost independent of the sign of α but in contrast with the relativistic case, they vanish for large values of ω. Once again, we can observe an apparent divergence as we approach the critical value ω_c.

The coordinates r_1 and r_2 describe the positions of the endpoints of the spring. We can simplify the Lagrangian by applying a suitable coordinate transformation:

$$\begin{aligned} X =& \frac{1}{2}(r_1 + r_2), \\ l =& r_2 - r_1. \end{aligned} \tag{1.30}$$

The inverse transformation is then:

$$\begin{aligned} r_1 =& X - \frac{l}{2}, \\ r_1 =& X + \frac{l}{2}. \end{aligned} \tag{1.31}$$

Since the two endpoints of the spring have the same mass, the coordinate X describes the position of the centre of mass of the body and l is the length of the dumbbell. We can now rewrite the Lagrangian of the system as:

$$L_s = \left(\frac{\mathrm{d}X}{\mathrm{d}t}\right)^2 + \frac{1}{4}\left(\frac{\mathrm{d}l}{\mathrm{d}t}\right)^2 + \frac{M}{X - \frac{l}{2}} + \frac{M}{X + \frac{l}{2}} - \frac{1}{2}k(l - l_0)^2. \tag{1.32}$$

We would like to simulate the fall of the glider with this model to better understand the behaviour in the critical regions. Therefore, we must select the parameters of the motion to be similar to the conditions of the glider. The spring should start in a compressed state when the two endpoints coincide, i.e., $l(0) = 0$. Without the gravitational field the spring would oscillate with an amplitude of the length $2l_0$. Therefore we set $l_0 = \delta l/2$. The total mechanical energy of the system is obviously conserved throughout the evolution.

The body will be dropped from $X(0) = R_0 = 120M$, starting from rest $\dot{X}(0) = \dot{l}(0) = 0$. We shall integrate the equations of motion for the spring numerically. Because the gravitational field influences the spring, the oscillations of the body are no longer harmonic. We can, however, control the speed of the relative motion of the endpoints of the spring indirectly through the rescaled spring constant k.

To compare the motion of the spring to the motion of the glider, one would like to wait until the spring shrinks back to a single point, stop the integration at this time and find the difference of the position of the spring in the gravitational field X and the position of a single mass dropped from the same height. Unfortunately, this is not possible because in the presence of the inhomogeneous gravitational field with the initial conditions described above the spring never shrinks back to a single point.

We have to think of a different condition for ending the integration of the equations of motion. We are looking for the first local minimum of the length of the spring after the first expansion, in other words, we are going to check if $\dot{l}(t) = 0$ and at the same time $\ddot{l}(t) \geq 0$. If these conditions are met, we stop the integration and we denote the time at this point as t_f.

Finally, we evaluate $X(t_f)$ and subtract the position of a free-falling point at the time t_f. We denote this quantity as the position shift δr. The desired result of this computation is the comparison of this dependence with Figure 1.9. However, our independent variable in this case is not a frequency parameter ω but the spring constant k. We shall therefore define $\omega(k) = 1/t_f(k)$ and plot the dependence of δr on this parameter ω. We also plot the inverse dependence $k = k(\omega)$ in Figures 1.11 and 1.12.

It is obvious that the position shift and the differential velocity depend on the parameter ω in a similar manner as in the case of the Newtonian glider and are always negative. The magnitude of the shifts is similar in both cases, too. This confirms that the existence of the swinging effect in the Newtonian case can be achieved even in this energy-conserving model. Once again, there is an apparent divergence for small values of ω. In this case, we understand much better the physical nature of the existence of a specific critical value of the spring constant. The parameter ω is controlled through k. A smaller value of the spring constant results in a smaller value of ω. However, a weaker spring is also less efficient in pulling the endpoints of the spring back together.

If we try to achieve an arbitrarily small value of ω, we hit a critical spring constant k_c, where the spring is no longer able to start contracting after it expands for the first time. If we choose a spring constant smaller than this critical value, the body will always expand, the conditions for stopping the integration are never satisfied and the lower endpoint of the body will eventually reach the gravitational centre. We show this behaviour in Figure 1.13. We found the critical value of the spring constant by the method of bisection. We were looking for a local minimum of the length of the spring in time. If such a minimum exists, the spring constant is above the critical value. On the other hand, if there is no local minimum, the

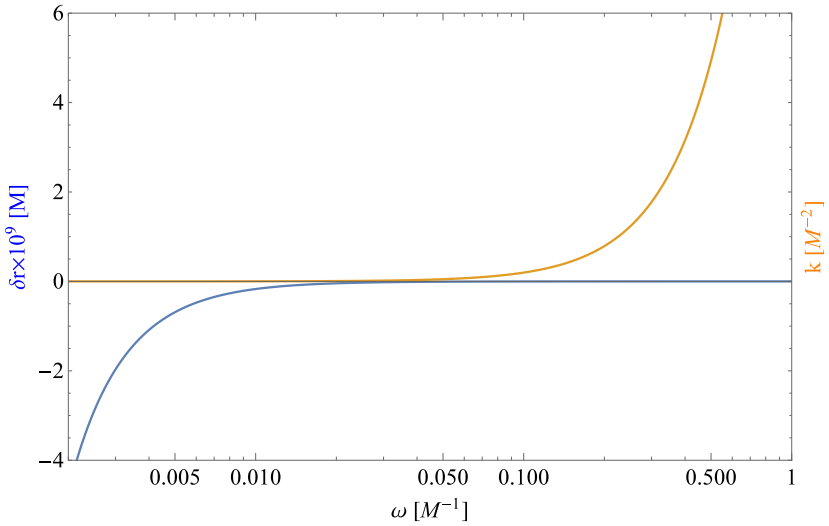

Figure 1.11: Dependence of the position shift of the cente of mass of a spring on the parameter ω. In this case, ω is not a free parameter of the motion, we can only control it through the spring constant k. The inverse of this dependence is also presented in this figure. Similarly to the glider model, there is an apparent divergence for small values of the parameter ω and the shift vanishes for large k and ω.

spring always expands and the chosen value is below the critical value. We found the critical value of the scaled spring constant k for the chosen starting position and rest length to be $k_c \doteq 5.8 \times 10^{-6} M^{-2}$.

This critical spring constant k_c corresponds to a critical spring constant ω, which does not have an analogy in the model with the glider. The engine deforming the glider can change its power and thus it will always pull the endpoints of the body back together. While doing that, the engine will however exert a mechanical force on the body and change its total mechanical energy at the expense of its own power source. In the following section, we study the dependence of this work done by the engine on the parameter ω.

1.5 Mechanical energy of the dumbbell glider

As we saw in the previous chapter, a simple Newtonian model predicts that a dumbbell interacting via a massless spring falling in a central gravitational field never shrinks back to a single point. The glider model with controlled Lagrangian on the other hand prescribes that the two masses coincide after the maneuver. The glider, therefore, acts as a spring with a varying spring constant.

This fact also suggests that the total mechanical energy of the glider probably isn't conserved. Let us explore this hypothesis. The total conserved mechanical

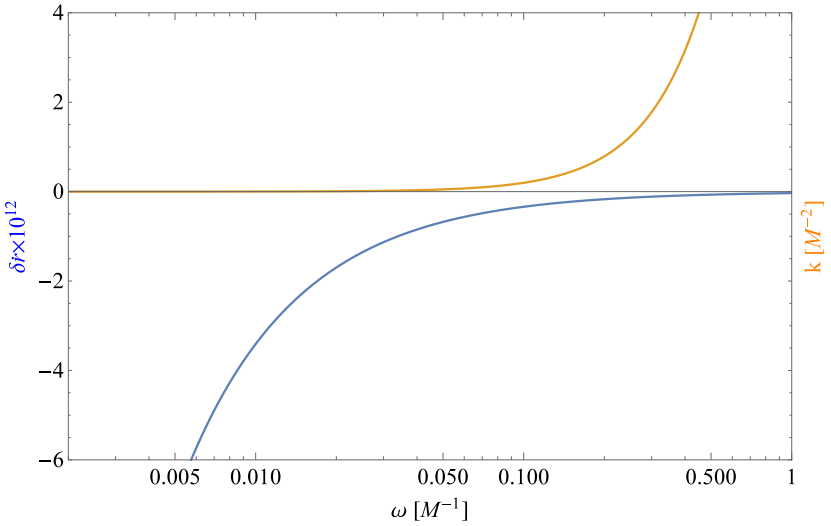

Figure 1.12: Dependence of the differential velocity of the centre of mass of a spring on the parameter ω. The course of the function $\delta\dot{r} = \delta\dot{r}(\omega)$ is once again very similar to the glider model.

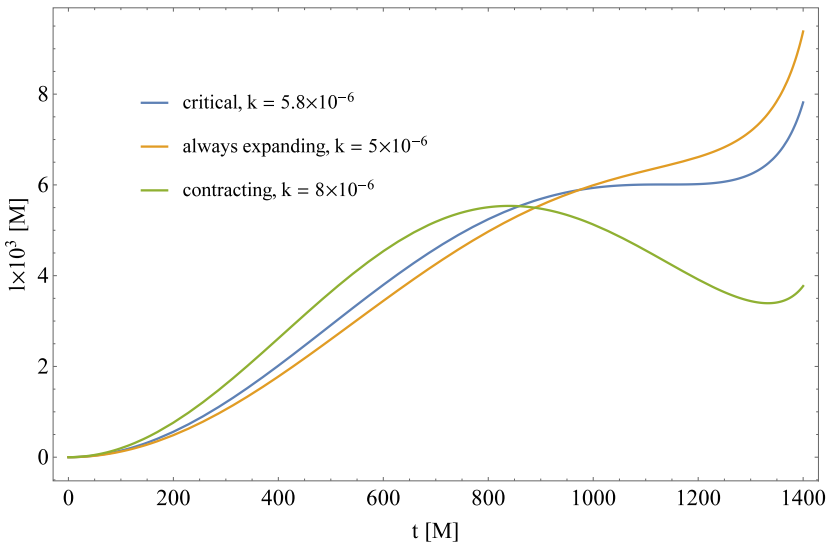

Figure 1.13: Time evolution for three chosen values of the rescaled spring constant k. There exists a critical value $k_c \doteq 5.8 \times 10^{-6} M^{-2}$ of the spring constant. If we study the fall of a spring with a lower spring constant, the spring will always expand and there is no relevant time when we should compare its position to the free-falling point.

energy for a radially falling Newtonian test particle is:

$$E_N = \frac{1}{2}m\left(\frac{\mathrm{d}r_p}{\mathrm{d}t}\right)^2 - \frac{Mm}{r_p}. \tag{1.33}$$

We define the total mechanical energy of the dumbbell as the sum of such terms for both endpoints. At the end of the stroke, both endpoints have the same energy because of the properties of the deformation function enforcing a zero relative velocity of the endpoints. Therefore, the total energy is simply twice that of the lower endpoint.

In the relativistic case, geodesic motion conserves the projection of the four-momentum on the timelike Killing vector field $\xi^\mu_{(t)}$:

$$E_r = -g_{\mu\nu}p^\mu\xi^\nu_{(t)} = -m\frac{\mathrm{d}t}{\mathrm{d}\tau}g_{tt}. \tag{1.34}$$

However, we chose the time coordinate t as the independent variable, which means that we have to express the zeroth component of the four-velocity. We can use the normalization condition of the four-velocity:

$$\begin{aligned} g_{tt}\left(\frac{\mathrm{d}t}{\mathrm{d}\tau}\right)^2 + g_{rr}\left(\frac{\mathrm{d}r}{\mathrm{d}\tau}\right)^2 = \\ = \left(\frac{\mathrm{d}t}{\mathrm{d}\tau}\right)^2\left[g_{tt} + g_{rr}\left(\frac{\mathrm{d}r}{\mathrm{d}t}\right)^2\right] = -1. \end{aligned} \tag{1.35}$$

From this we can express:

$$\frac{\mathrm{d}t}{\mathrm{d}\tau} = \frac{1}{\sqrt{-g_{tt} - g_{rr}\left(\frac{\mathrm{d}r}{\mathrm{d}t}\right)^2}}. \tag{1.36}$$

Finally, we obtain a formula for the energy of the test particle with t as an independent variable:

$$E_r = \frac{-mg_{tt}}{\sqrt{-g_{tt} - g_{rr}\left(\frac{\mathrm{d}r_p}{\mathrm{d}t}\right)^2}}. \tag{1.37}$$

For the Schwarzschild spacetime, this quantity is equal to:

$$E_r = \frac{m\left(1 - \frac{2M}{r_p}\right)}{\sqrt{1 - \frac{2M}{r_p} - \frac{\left(\frac{\mathrm{d}r_p}{\mathrm{d}t}\right)^2}{1 - \frac{2M}{r_p}}}}. \tag{1.38}$$

The calculated energy variations for the relativistic and Newtonian cases are presented in Figures 1.14 and 1.15, respectively. We can see that the energy of the system grows in the process. This means that the bond has to add mechanical energy to the system. More importantly, the energy input diverges in the critical regions. The glider would require an infinite energy source to execute the maneuver. The glider model is not sufficient in these critical regions.

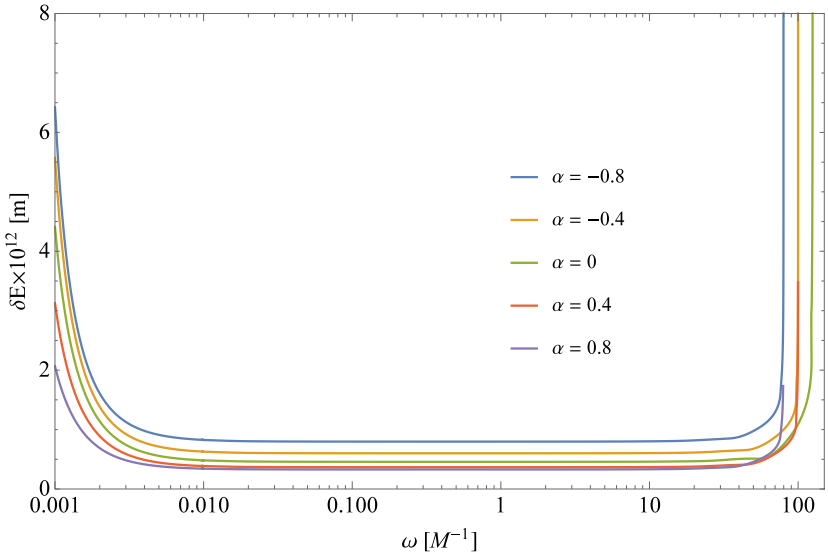

Figure 1.14: Variation of the mechanical energy of the relativistic glider after a single stroke. The energy input from the engine diverges in the critical regions of large and small values of the parameter ω. Since the position shift in the critical regions is negative, the gravitational energy of the dumbbell is smaller than that of a free particle. This means that the relevant contribution to the change of the mechanical energy comes from the kinetic part, which indicates that the dumbbell is approaching the speed of light.

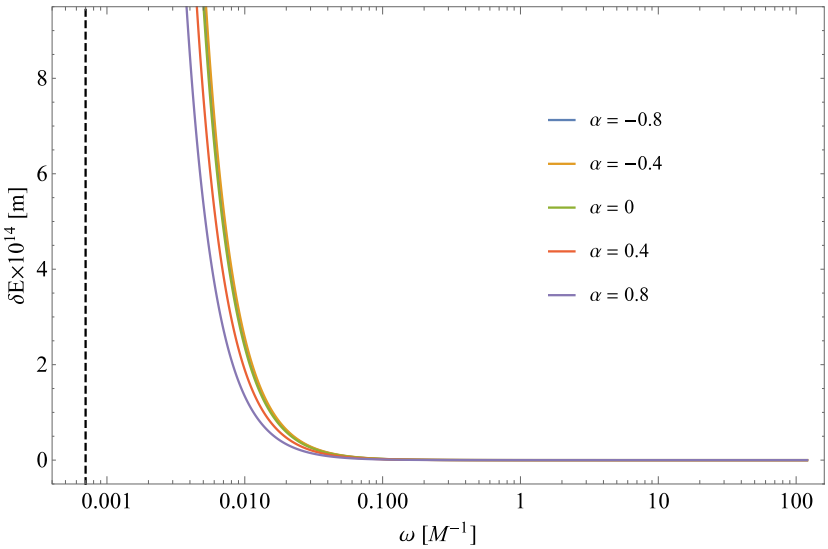

Figure 1.15: Variation of the mechanical energy of the Newtonian glider after a single stroke. The energy input diverges only for small ω's, there is no upper limit for ω in the studied interval.

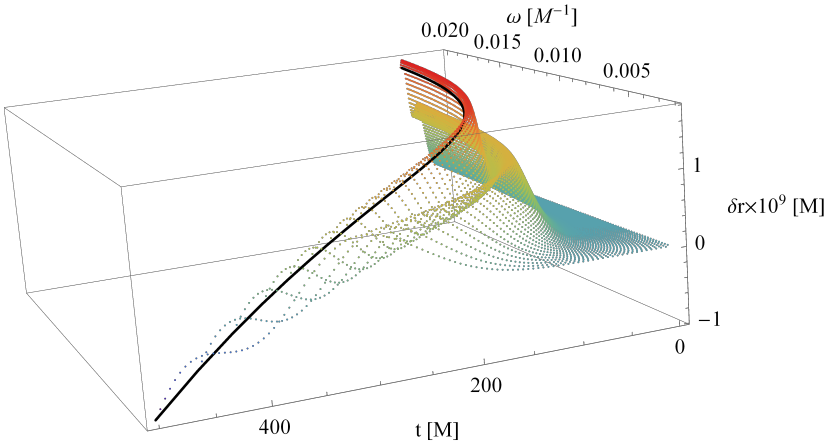

Figure 1.16: The position shift of the dumbbell in the relativistic case as a function of both t and ω. The edge of the 2D surface highlighted in black corresponds to the projected plot $\delta r(\omega)$. The apparent divergence is partially caused by the increasing time interval of the evolution of the body with decreasing ω.

1.6 Apparent divergence of the position shifts in the low-frequency region

In the previous chapter we could clearly see that the presence of apparent divergences is linked to the fact that the model acquires an infinite energy in the critical regions. If the body approaches the gravitational centre in the Newtonian case, the gravitational force becomes infinite and thus the engine must compensate this force in order to maintain the prescribed length of the body.

In the relativistic case, if our parameter approaches the critical value ω_c, the parts of the body are pushed near the speed of light and, once again, the engine must exert arbitrarily large force to achieve this. Moreover, we can see the divergence of the energy input in the critical region of small ω's in the relativistic case as well.

However, from Figure 1.7 it is obvious that the low-ω divergence is quicker than the one near the upper limit of the achievable values. This is because in this case, there are two factors at play. Apart from the energy input, there is a purely geometrical reason for the divergence.

The position shift as defined by 1.3 is a function of both t and ω. However, in the final plots we only show $\delta r = \delta r(\omega, t = 1/\omega)$. Then, the slope of this projection is given by:

$$\frac{\mathrm{d}}{\mathrm{d}\omega}\delta r(\omega) = \frac{\partial}{\partial\omega}\delta r(t,\omega)\bigg|_{t=\frac{1}{\omega}} - \frac{\partial}{\partial t}\delta r(t,\omega)\bigg|_{t=\frac{1}{\omega}} \frac{1}{\omega^2}. \tag{1.39}$$

Because the partial time derivative is negative, the second term drives the positive divergence of the slope in the projection. In Figure 1.16, we can see the full 3D plot of δr and the projected line.

To conclude, the presence of an apparent divergence in the low-frequency region

is influenced by this geometrical effect. We can expect this kind of behaviour for many similar models if we study the net displacements as a function of a "frequency" parameter. The glider model of [14] predicts unphysical behaviour of the bond because it requires infinite energy input in the critical regions. It is thus desirable to find a model of an oscillating body which satisfies the conservation of energy as well as the causality conditions.

2. Dixon's formalism for extended bodies and its applications

We showed in the previous chapter that the total mechanical energy of the two endpoints of the glider [14] is not conserved. Moreover, in the critical regions of the parameter ω the energy input grew divergently, which led us to the conclusion that the glider model is not applicable since we want to model an isolated body whose parts only act on one another and do not gain any energy from the outside or lose it. This means that the body can only store energy in the potential of the bond.

The example with a spring in a Newtonian gravitational field shows that the mechanical energy of the endpoints can change if the energy of the bond changes. One could therefore ask whether it is possible to assign some form of a potential or kinetic energy to the bond which would be conserved and which would explain the motion of the endpoints and the position shift.

In order to answer this question, we have to develop a framework which will allow us to analyse the motion of an extended body described by a general stress-energy tensor. This leads us to the theory of extended bodies developed by William Graham Dixon.

In the 1970s, Dixon published a series of papers [8-10] in which he found a system of equations describing any extended body described by a conserved symmetric stress-energy tensor. This scheme involves a set of differential equations for the evolution of the momenta of the tensor. The first paper in the series shows how to define the total four-momentum and the spin tensor of an extended body as observed by an arbitrary observer.

In the following papers in the series, Dixon goes on to define the forces acting on the extended body in an external gravitational and electro-magnetic fields. He thus obtains a full set of evolution equations for the momenta.

We are mostly interested in the results of the first paper in the series because it also shows several important results for extended bodies moving in maximally symmetric spacetimes, i.e., the de Sitter and anti-de Sitter universes. Because the presented description and the results may not be known to the reader, we shall derive Dixon's prediction for a body in a maximally symmetric spacetime with our choice of the signature of the metric and the Ricci identity.

In the second half of this chapter, we shall explore how one can apply Dixon's formalism to the problem of a system of test particles moving in a given gravitational background. Finally, we shall confront the results of Dixon's theory with the predictions of the glider model in maximally symmetric spacetimes.

2.1 The theory of bitensors

In this first section we shall discuss the definition and properties of bitensors as set by Synge [21] and DeWitt and Brehme [22]. This theory will help us develop an approach to extended bodies laid out by Dixon. Let us consider a manifold $\mathcal{M}$. A biscalar is a function defined for a set of ordered pairs of points $(x, z) \in \mathcal{M}$. Similarly, a bitensor is an object defined at two points of the manifold which transforms as a tensor with the change of the coordinate system near one of the points.

An example of a biscalar is the world function biscalar. We only consider such ordered pairs of points in the spacetime (x, z) which can be uniquely connected by a geodesic $x(u)$. The world function biscalar is defined as:

$$\sigma(x,z) = \frac{1}{2}(u_2 - u_1)\int_{u_1}^{u_2}\left[-g_{\alpha\beta}(x(u))\frac{\mathrm{d}x^\alpha}{\mathrm{d}u}\frac{\mathrm{d}x^\beta}{\mathrm{d}u}\right]\mathrm{d}u, \tag{2.1}$$

where the integral is calculated along the geodesic connecting the two points. This definition is independent of the chosen affine parametrization of the geodesic. The endpoints of the geodesic are chosen as: $x = x(u_1)$ and $z = x(u_2)$. One has to distinguish which tensor indices belong to which of the pair of points. To this end, we shall use the indices $\alpha, \beta, ...$ at the point x and the indices $\kappa, \lambda, ...$ at the point z. We denote the derivatives of the world function biscalar simply by adding the indices:

$$\sigma_{\alpha\beta\kappa}(x,z) = \nabla_\kappa \nabla_{\beta\alpha}\sigma(x,z). \tag{2.2}$$

We can notice that the covariant derivatives at the point x commute with those at z for any bitensor.

The integral in 2.1 is extremal for perturbations of the path between the fixed points x, z. This means that if we perturb the path $x(u)$ including the endpoints, the perturbation in the biscalar will be:

$$\delta\sigma = (u_2 - u_1)\left[-g_{\mu\nu}(x(u))\frac{\mathrm{d}x^\mu}{\mathrm{d}u}\delta x^\nu(u)\right]_{u_1}^{u_2}. \tag{2.3}$$

At the same time:

$$\delta\sigma = \frac{\partial\sigma}{\partial x^\mu}\delta x^\mu + \frac{\partial\sigma}{\partial z^\mu}\delta z^\mu. \tag{2.4}$$

Comparing these expressions together, we get:

$$\begin{aligned}\frac{\partial\sigma}{\partial x^\alpha} &= (u_2 - u_1)g_{\alpha\beta}(x)\dot{x}^\beta(u_1),\\ \frac{\partial\sigma}{\partial z^\kappa} &= -(u_2 - u_1)g_{\kappa\lambda}(z)\dot{x}^\lambda(u_2).\end{aligned} \tag{2.5}$$

We represent the tangent vector of the geodesic by $\dot{x}^\alpha$. We can use our index notation to distinguish the tangent vector at the two endpoints. Moreover, we choose the special parametrization $u_1 = 0$, $u_2 = u$. Thus, the relations can be written in the compact form:

$$\begin{aligned}\sigma^\alpha &= u\dot{x}^\alpha,\\ \sigma^\kappa &= -u\dot{x}^\kappa.\end{aligned} \tag{2.6}$$

The norm of the tangent vector does not change along a geodesic. This means that the argument of the integral in 2.1 is a constant and thus the integral can be easily calculated.

$$\sigma(x,z) = -\frac{1}{2}u^2 g_{\alpha\beta}\dot{x}^\alpha \dot{x}^\beta. \tag{2.7}$$

Consequently, we can express:

$$2\sigma = -\sigma_\kappa \sigma^\kappa = -\sigma_\alpha \sigma^\alpha. \tag{2.8}$$

We can see that σ^α is a vector at x tangent to the geodesic connecting x and z. The length of this vector is equal to the that of the geodesic. This vector is a natural generalization of the position vector of z relative to x from the Minkowski spacetime.

2.2 Extended bodies in Dixon's theory

Dixon's formalism describes the motion of extended bodies in general relativity through a set of differential equations for different moments of the body. The interpretation of the results can also help us understand better what we should expect in specific cases of extended bodies such as a system of interacting particles. In general, Dixon's formalism allows an interaction of the body with an external electromagnetic field. For simplicity, we shall only assume an electrically neutral body in a gravitational field.

The extended body is described by a symmetric stress-energy tensor $T^{\alpha\beta}$ defined on the spacetime $(\mathcal{M}, g)$, which satisfies the conservation laws:

$$T^{\alpha\beta}{}_{;\beta} = 0. \tag{2.9}$$

We also have to assume that the body is finite in the sense that the support of $T^{\alpha\beta}$ is a worldtube W, which satisfies the following condition: the intersection of an arbitrary hypersurface Σ with W lies in an open set N of $\mathcal{M}$ which is a normal neighbourhood of each of its points, and whose inverse image under the exponential map at any point $p \in N$ is bounded. This rather complicated condition ensures that the body is finite in the spatial dimensions and that the spacelike geodesics within the body are well-behaved. For further details and the definition of a normal neighbourhood see [23].

The formalism does not require the extended body to be a test body, the stress-energy tensor can be the source side of the Einstein equations or its part.

Assume that there is a Killing vector field ξ^α in the spacetime, i.e.:

$$\mathcal{L}_\xi g_{\alpha\beta} = \xi_{\alpha;\beta} + \xi_{\beta;\alpha} = 2\xi_{(\alpha;\beta)} = 0. \tag{2.10}$$

$\mathcal{L}_\xi$ denotes the Lie derivative along the vector field ξ^α. We can easily see that:

$$\nabla_\beta (T^{\alpha\beta}\xi_\alpha) = 0. \tag{2.11}$$

Let Σ be an arbitrary spacelike hypersurface. Let us define the scalar function:

$$\mathcal{G}(\Sigma) = \int_\Sigma T^{\alpha\beta}\xi_\alpha\sqrt{-g}\mathrm{d}\Sigma_\beta. \tag{2.12}$$

Because the body is finite in the spatial directions, the application of the Stokes's theorem gives the independence of $\mathcal{G}$ on the choice of particular hypersurface Σ. This quantity is therefore a constant of motion for the extended body.

2.3 Integrating the geodesic deviation equation

In this section, we shall show how the theory of bitensors can be used to integrate the equation of geodesic deviation. Consider once again a Killing vector field ξ^α and any geodesic $x(u)$. Using 2.10 and the Ricci identity for covectors, it can be easily shown by permuting the indices that the Killing field satisfies:

$$\xi_{\alpha;\beta\gamma} + R^\mu{}_{\gamma\alpha\beta}\xi_\mu = 0, \tag{2.13}$$

where $R^\mu{}_{\gamma\alpha\beta}$ is the Riemann tensor. Multiplying this equation twice by the tangent vector $\dot{x}^\beta$ of the geodesic, we get:

$$\frac{\mathrm{D}^2\xi_\alpha}{\mathrm{d}u^2} + R^\mu{}_{\gamma\alpha\beta}\dot{x}^\beta\dot{x}^\gamma\xi_\mu = 0. \tag{2.14}$$

This is the equation of geodesic deviation. The solution is determined by specifying the initial value $\xi_\alpha(0)$ and the first derivative $\mathrm{D}\xi_\alpha/\mathrm{d}u$ at one point of the geodesic $x(u=0)$. From 2.10, we can also easily obtain:

$$\frac{\mathrm{D}\xi_\alpha}{\mathrm{d}u} = \dot{x}^\beta\xi_{[\alpha;\beta]}. \tag{2.15}$$

Now consider the set of all points which can be uniquely connected with $x = x(0)$ by a geodesic. For given initial values of ξ_α and $\xi_{[\alpha;\beta]}$, we can use the equations 2.15 and 2.14 to define a vector field in all points of a normal neighbourhood of x.

Now consider a 1-parameter class of geodesics $x(u,v)$ with the affine parameter u, where v labels the different geodesics. We shall denote:

$$\begin{aligned}\dot{x}^\alpha &= \frac{\partial x^\alpha}{\partial u},\\ \eta^\alpha &= \frac{\partial x^\alpha}{\partial v}.\end{aligned} \tag{2.16}$$

We know that η^α then satisfies the geodesic deviation equation 2.14. From the theory of bitensors we know that:

$$\sigma^\alpha(x(0,v), x(u,v)) = u\dot{x}^\alpha, \tag{2.17}$$

where we used our index notation to distinguish the derivatives at $x(0,v)$ and those at $x(u,v)$. Applying a covariant derivative with respect to v to this equations gives us:

$$\sigma^\alpha{}_\lambda\eta^\lambda + \sigma^\alpha{}_\beta\eta^\beta = u\frac{\mathrm{D}\dot{x}^\alpha}{\mathrm{d}v}. \tag{2.18}$$

From 2.16:

$$\frac{\mathrm{D}\dot{x}^\kappa}{\mathrm{d}v} = \frac{\mathrm{D}\eta^\kappa}{\mathrm{d}u}. \tag{2.19}$$

We also define the inverse matrix ${}^{-1}\sigma^\kappa{}_\alpha$ satisfying:

$${}^{-1}\sigma^\kappa{}_\alpha \sigma^\alpha{}_\lambda = \delta^\kappa_\lambda. \tag{2.20}$$

We can use this to rewrite 2.18 as:

$$\eta^\kappa = -{}^{-1}\sigma^\kappa{}_\alpha \sigma^\alpha{}_\beta \eta^\beta + u\,{}^{-1}\sigma^\kappa{}_\alpha \frac{\mathrm{D}\eta^\alpha}{\mathrm{d}u}. \tag{2.21}$$

For $v = 0$, this gives us the solution of the geodesic deviation equation 2.14 along the geodesic $x(u, 0)$ from an initial value and derivative of η^α at $x(0, 0)$. But we can choose the geodesic $x(u)$ arbitrarily and, therefore, we can define the vector field by this relation in the whole normal neighbourhood of $x(0)$.

For convenience, we define:

$$\begin{aligned} K^\kappa{}_\alpha &= -\,{}^{-1}\sigma^\kappa{}_\beta \sigma^\beta{}_\alpha \\ H^\kappa{}_\alpha &= {}^{-1}\sigma^\kappa{}_\alpha. \end{aligned} \tag{2.22}$$

Then we can rewrite 2.21 as:

$$\eta^\kappa = K^\kappa{}_\alpha \eta^\alpha + u H^\kappa{}_\alpha \frac{\mathrm{D}\eta^\alpha}{\mathrm{d}u}. \tag{2.23}$$

Finally, when we apply this to the case of a Killing vector field, we obtain:

$$\xi_\kappa = K_\kappa{}^\alpha \xi_\alpha + H_\kappa{}^\alpha \sigma^\beta \xi_{[\alpha;\beta]}. \tag{2.24}$$

2.4 Extended body in a maximally symmetric spacetime

In this section, we shall define the four-momentum and the spin tensor for an extended body moving in a maximally symmetric spacetime, i.e., the (anti-)de Sitter universe or the trivial case of the Minkowski spacetime. The conservation laws then imply the existence of a worldline with special properties, whose physical interpretation will be obvious.

We begin by choosing an arbitrary hypersurface Σ and any point $x \in W \cap \Sigma$. Then, using our assumptions, 2.24 holds everywhere in $W \cap \Sigma$. We define the four-momentum and the spin tensor of the extended body relative to x as:

$$p^\alpha(x, \Sigma) = \int_\Sigma K_\kappa{}^\alpha T^{\kappa\lambda} \sqrt{-g}\mathrm{d}\Sigma_\lambda, \tag{2.25}$$

$$S^{\alpha\beta}(x, \Sigma) = 2\int_\Sigma \sigma^{[\beta} H_\kappa{}^{\alpha]} T^{\kappa\lambda} \sqrt{-g}\mathrm{d}\Sigma_\lambda. \tag{2.26}$$

These objects transform as a vector and a tensor at the point x, respectively. We can rewrite the constant of motion 2.12 using these definitions as a product of tensors defined at x:

$$\mathcal{G} = p^\alpha \xi_\alpha + \frac{1}{2} S^{\alpha\beta} \xi_{[\alpha;\beta]}. \tag{2.27}$$

Since we know that $\mathcal{G}$ does not depend on the point x or the hypersurface Σ, we can restrict the dependence of p^α and $S^{\alpha\beta}$. We choose a foliation of the spacetime $\Sigma(s)$ and a worldline $x(s)$ such that $x(s) \in W \cap \Sigma(s)$. For the moment, we can even consider spacelike or null worldlines and we do not require s to be the proper interval along the worldline. The four-momentum and the spin tensor are defined along $x(s)$ and thus we can differentiate 2.27 with respect to s. Denoting $v^\alpha = \mathrm{d}x^\alpha/\mathrm{d}s$ and using 2.13, we get:

$$\xi_\alpha \left[\frac{\mathrm{D}p^\alpha}{\mathrm{d}s} - \frac{1}{2} S^{\beta\gamma} R^\alpha{}_{\delta\beta\gamma} v^\delta \right] + \frac{1}{2} \xi_{[\alpha;\beta]} \left[\frac{\mathrm{D}S^{\alpha\beta}}{\mathrm{d}s} + 2p^{[\alpha} v^{\beta]} \right] = 0. \tag{2.28}$$

This equation must hold for any choice of the Killing vector field. If the spacetime is maximally symmetric, the values of ξ_α and $\xi_{[\alpha;\beta]}$ can be arbitrary and thus the expressions in the brackets have to vanish for any choice of the foliation and the worldline.

$$\frac{\mathrm{D}p^\alpha}{\mathrm{d}s} = \frac{1}{2} S^{\beta\gamma} R^\alpha{}_{\delta\beta\gamma} v^\delta, \tag{2.29}$$

$$\frac{\mathrm{D}S^{\alpha\beta}}{\mathrm{d}s} = -2p^{[\alpha} v^{\beta]}. \tag{2.30}$$

The Riemann tensor in the maximally symmetric spacetime can be expressed as:

$$R_{\alpha\beta\gamma\delta} = k(g_{\alpha\gamma} g_{\beta\delta} - g_{\alpha\delta} g_{\beta\gamma}) \tag{2.31}$$

and thus the first equation takes the form:

$$\frac{\mathrm{D}p^\alpha}{\mathrm{d}s} = k S^{\alpha\beta} v_\beta. \tag{2.32}$$

These equations can be integrated along the chosen worldline from the initial values of p^α and $S^{\alpha\beta}$ at the point x. This means that the particular choice of the foliation $\Sigma(s)$ does not matter. We could have also used any worldline $x(s)$, therefore, as a vector and tensor fields, the four-momentum and the spin tensor have to satisfy the equations:

$$p_{\alpha;\beta} = k S_{\alpha\beta}, \tag{2.33}$$

$$S_{\alpha\beta;\gamma} = -2p_{[\alpha} g_{\beta]\gamma}. \tag{2.34}$$

The first equation shows that p^α is a Killing vector field and thus it satisfies 2.13. But then for $k \neq 0$, 2.33 implies 2.34. This means that the only restriction on p^α is that it is a Killing vector field and after the choice of p^α, the equation 2.33 can be used to calculate $S^{\alpha\beta}$, which identically satisfies 2.34.
Let us assume that there is a point x_0 where:

$$p^\alpha p_{\beta;\alpha} = 0. \tag{2.35}$$

Then for $k \neq 0$ by 2.33 also:

$$p_\alpha S^{\alpha\beta} = 0. \tag{2.36}$$

Denote L_0 the integral curve of the Killing field p^α going through x_0. Then 2.35 will hold along L_0 and L_0 is a geodesic with the tangent vector p^α. Moreover, the

magnitude of the vector does not change.

The dominant energy condition for $T^{\alpha\beta}$ is sufficient for the existence of the point x_0 satisfying 2.35 [8]. Dixon goes on to prove that this worldline is then unique except for one special case, which we shall not discuss here. Let us only state that this case is not physically relevant. The single remaining worldline is also timelike and can be associated with the centre of mass of the extended body. In maximally symmetric spacetimes, the centre of mass thus moves along a geodesic. This answers our question about possible swimming effects in these cases: if we define the centre of mass according to this definition then the net displacement of the centre of mass with respect to a geodesic motion with the same initial conditions vanishes unless the conservation laws are violated, i.e., unless the system loses or gains energy.

The evolution equations for the four-momentum and the spin tensor along L_0 reduce to:

$$\frac{\mathrm{D}p^\alpha}{\mathrm{d}s} = 0, \tag{2.37}$$

$$\frac{\mathrm{D}S^{\alpha\beta}}{\mathrm{d}s} = 0. \tag{2.38}$$

2.5 The stress-energy tensor of a test particle

In the previous sections we saw how the conservation laws restrict the motion of an extended body described by a general stress-energy tensor. In this section, we apply the results to the case of a set of test particles moving on a given background. To this end, we have to find a stress-energy tensor of such a system.

The stress-energy tensor can be derived from the Lagrangian. Let us consider a single test particle. We shall use the action for the trajectory parametrized by the coordinate time $x^0 = t$. The trajectory is $z^\mu(t)$. We justify using the coordinate time as the independent variable in Chapter 3. The action for the geodesic motion is:

$$S_p = -m \int \sqrt{-g_{\alpha\beta} \frac{\mathrm{d}z^\alpha}{\mathrm{d}t} \frac{\mathrm{d}z^\beta}{\mathrm{d}t}} \mathrm{d}t. \tag{2.39}$$

To find the stress-energy tensor, we need to find the Lagrangian density. We have to add the integration over the spatial coordinates. Moreover, the invariant volume element has to be multiplied by the square root of the negative determinant of the metric tensor. The action then takes the form:

$$S_p = -m \int \left[\frac{1}{\sqrt{-g}} \sqrt{-g_{\alpha\beta}(z(t)) \frac{\mathrm{d}z^\alpha}{\mathrm{d}t} \frac{\mathrm{d}z^\beta}{\mathrm{d}t}} \delta^{(3)}(\vec{x} - \vec{z}(t)) \right] \sqrt{-g} \mathrm{d}^4 x. \tag{2.40}$$

The vectors represent the spatial coordinates, g is the determinant of the metric tensor and, finally, $\delta^{(3)}$ is the three-dimensional delta distribution. The Lagrangian density for the free test particle then is:

$$\mathcal{L}_p = -\frac{m}{\sqrt{-g}} \sqrt{-g_{\alpha\beta}(z(t)) \frac{\mathrm{d}z^\alpha}{\mathrm{d}t} \frac{\mathrm{d}z^\beta}{\mathrm{d}t}} \delta^{(3)}(\vec{x} - \vec{z}(t)). \tag{2.41}$$

By definition, the stress-energy tensor can be obtained in the following form:

$$T_{\mu\nu} = -\frac{2}{\sqrt{-g}} \frac{\partial \left(\sqrt{-g}\mathcal{L}_p\right)}{\partial g^{\mu\nu}}. \tag{2.42}$$

By differentiating the equation $g^{\alpha\rho}g_{\rho\beta} = \delta^{\alpha}_{\beta}$ we find the formula:

$$\frac{\partial g_{\mu\nu}}{\partial g^{\alpha\beta}} = -g_{\mu\alpha}g_{\nu\beta}. \tag{2.43}$$

We can now easily find the stress-energy tensor of the test particle:

$$T^{\mu\nu} = \frac{m}{\sqrt{-g}} \frac{\dfrac{\mathrm{d}z^{\mu}}{\mathrm{d}t}\dfrac{\mathrm{d}z^{\nu}}{\mathrm{d}t}}{\sqrt{-g_{\alpha\beta}(z(t))\dfrac{\mathrm{d}z^{\alpha}}{\mathrm{d}t}\dfrac{\mathrm{d}z^{\beta}}{\mathrm{d}t}}} \delta^{(3)}(\vec{x} - \vec{z}(t)). \tag{2.44}$$

2.6 Conservation laws for the test particle

The key assumption of Dixon's theory of extended bodies is that the stress-energy tensor satisfies the conservation laws:

$$T^{\mu\nu}{}_{;\nu} = 0. \tag{2.45}$$

The conservation laws are in general four differential equations for the system. We can ask whether they are equivalent to the equations of motion and whether they fully determine the evolution of the system. For example, if $T^{\mu\nu}$ is the stress-energy tensor of the electromagnetic field, the conservation laws are equivalent to the first set of Maxwell's equations. A general antisymmetric tensor in four dimensions has 6 independent components. Thus if we use the tensor of the electromagnetic field as the field variable, the 4 conservation laws do not fully determine the evolution. However, if we accept the existence of the four-potential and treat it as the right field variable, the conservation laws are sufficient.

Similarly, the conservation laws for the perfect fluid imply the continuity equation as well as the Euler equation for the fluid. However, they do not restrict the equation of state of the fluid. If we treat the pressure as a separate variable, the conservations laws do not fully describe the evolution of the system.

Let us inspect how much the conservation laws for the test particle restrict its motion. We can express the four-divergence in the following form:

$$T^{\mu\nu}{}_{;\nu} = \frac{1}{\sqrt{-g}} \left(\sqrt{-g}T^{\mu\nu}\right)_{,\nu} + \Gamma^{\mu}{}_{\nu\sigma}T^{\nu\sigma}. \tag{2.46}$$

From 2.44 we can evaluate:

$$\begin{aligned}
\frac{1}{m}\left(\sqrt{-g}T^{\mu\nu}\right)_{,\nu} &= \left(\frac{\frac{\mathrm{d}z^\mu}{\mathrm{d}t}\frac{\mathrm{d}z^\nu}{\mathrm{d}t}\delta^{(3)}(\vec{x}-\vec{z}(t))}{\sqrt{-g_{\alpha\beta}(z(t))\frac{\mathrm{d}z^\alpha}{\mathrm{d}t}\frac{\mathrm{d}z^\beta}{\mathrm{d}t}}}\right)_{,\nu} \\
&= \left(\frac{\frac{\mathrm{d}z^\mu}{\mathrm{d}t}\delta^{(3)}(\vec{x}-\vec{z}(t))}{\sqrt{-g_{\alpha\beta}(z(t))\frac{\mathrm{d}z^\alpha}{\mathrm{d}t}\frac{\mathrm{d}z^\beta}{\mathrm{d}t}}}\right)_{,t} + \left(\frac{\frac{\mathrm{d}z^\mu}{\mathrm{d}t}\frac{\mathrm{d}z^i}{\mathrm{d}t}\delta^{(3)}(\vec{x}-\vec{z}(t))}{\sqrt{-g_{\alpha\beta}(z(t))\frac{\mathrm{d}z^\alpha}{\mathrm{d}t}\frac{\mathrm{d}z^\beta}{\mathrm{d}t}}}\right)_{,i} \\
&= -\sum_{i=1}^{3}\frac{\frac{\mathrm{d}z^\mu}{\mathrm{d}t}\delta^{(2)-i}(\vec{x}-\vec{z}(t))\delta'(x^i-z^i(t))\frac{\mathrm{d}z^i}{\mathrm{d}t}}{\sqrt{-g_{\alpha\beta}(z(t))\frac{\mathrm{d}z^\alpha}{\mathrm{d}t}\frac{\mathrm{d}z^\beta}{\mathrm{d}t}}} + \frac{\frac{\mathrm{d}^2z^\mu}{\mathrm{d}t^2}\delta^{(3)}(\vec{x}-\vec{z}(t))}{\sqrt{-g_{\alpha\beta}(z(t))\frac{\mathrm{d}z^\alpha}{\mathrm{d}t}\frac{\mathrm{d}z^\beta}{\mathrm{d}t}}} + \\
&+ \frac{\frac{\mathrm{d}z^\mu}{\mathrm{d}t}\left(\frac{1}{2}g_{\rho\sigma,\tau}\frac{\mathrm{d}z^\rho}{\mathrm{d}t}\frac{\mathrm{d}z^\sigma}{\mathrm{d}t}\frac{\mathrm{d}z^\tau}{\mathrm{d}t} + g_{\rho\sigma}\frac{\mathrm{d}^2z^\rho}{\mathrm{d}t^2}\frac{\mathrm{d}z^\sigma}{\mathrm{d}t}\right)}{\left(-g_{\alpha\beta}(z(t))\frac{\mathrm{d}z^\alpha}{\mathrm{d}t}\frac{\mathrm{d}z^\beta}{\mathrm{d}t}\right)^{\frac{3}{2}}}\delta^{(3)}(\vec{x}-\vec{z}(t)) + \\
&+ \sum_{i=1}^{3}\frac{\frac{\mathrm{d}z^\mu}{\mathrm{d}t}\delta^{(2)-i}(\vec{x}-\vec{z}(t))\delta'(x^i-z^i(t))\frac{\mathrm{d}z^i}{\mathrm{d}t}}{\sqrt{-g_{\alpha\beta}(z(t))\frac{\mathrm{d}z^\alpha}{\mathrm{d}t}\frac{\mathrm{d}z^\beta}{\mathrm{d}t}}}.
\end{aligned} \tag{2.47}$$

Here, δ' is the derivative of the delta distribution and $\delta^{(2)-i}$ is the two-dimensional delta distribution without the i-th dimension. The first and last terms in this expression cancel. The conservation laws take the form:

$$\begin{aligned}
T^{\mu\nu}{}_{;\nu} =& \frac{m}{\sqrt{-g}}\left[\frac{\frac{\mathrm{d}^2z^\mu}{\mathrm{d}t^2}}{\sqrt{-g_{\alpha\beta}(z(t))\frac{\mathrm{d}z^\alpha}{\mathrm{d}t}\frac{\mathrm{d}z^\beta}{\mathrm{d}t}}} + \Gamma^\mu{}_{\rho\sigma}\frac{\frac{\mathrm{d}z^\rho}{\mathrm{d}t}\frac{\mathrm{d}z^\sigma}{\mathrm{d}t}}{\sqrt{-g_{\alpha\beta}(z(t))\frac{\mathrm{d}z^\alpha}{\mathrm{d}t}\frac{\mathrm{d}z^\beta}{\mathrm{d}t}}} + \right. \\
&\left. + \frac{\frac{\mathrm{d}z^\mu}{\mathrm{d}t}\frac{1}{2}g_{\rho\sigma,\tau}\frac{\mathrm{d}z^\rho}{\mathrm{d}t}\frac{\mathrm{d}z^\sigma}{\mathrm{d}t}\frac{\mathrm{d}z^\tau}{\mathrm{d}t} + g_{\rho\sigma}\frac{\mathrm{d}^2z^\rho}{\mathrm{d}t^2}\frac{\mathrm{d}z^\sigma}{\mathrm{d}t}}{\left(-g_{\alpha\beta}(z(t))\frac{\mathrm{d}z^\alpha}{\mathrm{d}t}\frac{\mathrm{d}z^\beta}{\mathrm{d}t}\right)^{\frac{3}{2}}}\right]\delta^{(3)}(\vec{x}-\vec{z}(t)).
\end{aligned} \tag{2.48}$$

This means that if we want to satisfy the conservation laws, the expression in the brackets has to be equal to 0.

$$\frac{\mathrm{d}^2z^\mu}{\mathrm{d}t^2} + \frac{\frac{\mathrm{d}z^\mu}{\mathrm{d}t}\frac{1}{2}g_{\rho\sigma,\tau}\frac{\mathrm{d}z^\rho}{\mathrm{d}t}\frac{\mathrm{d}z^\sigma}{\mathrm{d}t}\frac{\mathrm{d}z^\tau}{\mathrm{d}t} + g_{\rho\sigma}\frac{\mathrm{d}^2z^\rho}{\mathrm{d}t^2}\frac{\mathrm{d}z^\sigma}{\mathrm{d}t}}{-g_{\alpha\beta}\frac{\mathrm{d}z^\alpha}{\mathrm{d}t}\frac{\mathrm{d}z^\beta}{\mathrm{d}t}} + \Gamma^\mu{}_{\rho\sigma}\frac{\mathrm{d}z^\rho}{\mathrm{d}t}\frac{\mathrm{d}z^\sigma}{\mathrm{d}t} = 0. \tag{2.49}$$

The general form of the non-affine parametrization of the geodesic equation is:

$$\frac{\mathrm{d}^2 z^\mu}{\mathrm{d}p^2} - \frac{\mathrm{d}z^\mu}{\mathrm{d}p}\frac{\frac{\mathrm{d}^2\tau}{\mathrm{d}p^2}}{\frac{\mathrm{d}\tau}{\mathrm{d}p}} + \Gamma^\mu{}_{\rho\sigma}\frac{\mathrm{d}z^\rho}{\mathrm{d}p}\frac{\mathrm{d}z^\sigma}{\mathrm{d}p} = 0, \tag{2.50}$$

where τ is the affine parameter and p is the non-affine parameter. In our case, we have:

$$\frac{\mathrm{d}\tau}{\mathrm{d}t} = \sqrt{-g_{\alpha\beta}\frac{\mathrm{d}z^\alpha}{\mathrm{d}t}\frac{\mathrm{d}z^\beta}{\mathrm{d}t}}. \tag{2.51}$$

This means that 2.49 is the geodesic equation parametrized by the coordinate time. The conservation laws for the stress-energy tensor of a free test particle are equivalent with the geodesic equation.

If we were studying a system of several independent test particles, the stress-energy tensor would be a sum of the individual terms 2.44. To satisfy the conservation laws, each particle has to move along a geodesic. However, the particles can decay or collide if they meet while preserving the total four-momentum during the process.

The glider model from Chapter 1 cannot satisfy such conservation laws during the gliding maneuver because the endpoints don't follow a geodesic. One could still hope that the conservation laws can be saved by somehow including the stress-energy tensor of the bond into the description. In the following section, we show that this is not possible.

2.7 The relativistic glider in the de Sitter universe

Dixon's theory predicts that in maximally symmetric spacetimes the centre of mass of any extended object described by its stress-energy tensor field, which satisfies conservation laws, moves along a geodesic and thus no swimming or swinging effect can be measured. Furthermore, this trajectory of the centre of mass with the desired properties is unique.

We shall use these results to test the glider model from Chapter 1 by applying a similar computation in the de Sitter and anti-de Sitter universes. The Lagrangian for a single test particle is:

$$L_p = -m\sqrt{1 - \frac{\Lambda}{3}r_p^2 - \frac{1}{1-\frac{\Lambda}{3}r_p^2}\left(\frac{\mathrm{d}r_p}{\mathrm{d}t}\right)^2}, \tag{2.52}$$

where Λ is the cosmological constant, which can be positive (de Sitter) or negative (anti-de Sitter). The coordinate time does not correspond to the proper time of a distant static observer. Not only that but in the de Sitter case, an asymptotic static observer is not even physical because there is a cosmological

horizon located at $r_H = \sqrt{3/\Lambda}$. However, the coordinate time can be associated with the proper time of a stationary observer at $r = 0$.

Similarly to the Schwarzschild spacetime, no object can cross the horizon in a finite coordinate time. The glider Lagrangian can be written in a similar manner:

$$\begin{aligned} L_d = &- m \sqrt{1 - \frac{\Lambda}{3} r_d^2 - \frac{1}{1 - \frac{\Lambda}{3} r_d^2} \left(\frac{\mathrm{d}r_d}{\mathrm{d}t} \right)^2} \\ &- m \sqrt{1 - \frac{\Lambda}{3} (r_d + l)^2 - \frac{1}{1 - \frac{\Lambda}{3} (r_d + l)^2} \left(\frac{\mathrm{d}r_d}{\mathrm{d}t} + \frac{\mathrm{d}l}{\mathrm{d}t} \right)^2}. \end{aligned} \tag{2.53}$$

The choice of the deformation function $l(t, \omega, \alpha)$ is the same as in Chapter 1. We once again integrate the equations of motion numerically for the duration of one stroke of the glider for different values of the parameters ω and α. We then compare the position shift δr and the differential velocity $\delta \dot{r}$ to a free test particle falling from the same position with the same initial four-momentum.

In our numerical computations, we choose the position of the horizon in the de Sitter case to be $r_H = 300$. This means that the length units are $r_H/300 = 1/\sqrt{30000 \mid \Lambda \mid}$. We used the same expression as the length scale also for the anti-de Sitter case. We denote this expression by L. We choose the initial position $R_0 = 120L$ and the initial coordinate velocity of the glider is 0. The maximal coordinate length of the glider is $\delta l = 5 \times 10^{-3} L$.

The results of the computations are shown in Figures 2.1, 2.2, 2.3 and 2.4. In the anti-de Sitter case we cannot use the smallest values of the parameter ω because the free particle and the glider reach $r = 0$ in a finite time and the coordinate system is singular there. We can see that the net displacements do not vanish at the end of the motion. We can also notice that the shift is positive for negative values of the asymmetry parameter α in the de Sitter universe. In this case the free object is driven towards the horizon and thus the position shift happens in the same direction as the total displacement of the body. One could ask whether we chose the correct geodesic to compare the net position of the glider. This has to be the case because the glider is a point object at the beginning.

This result directly contradicts Dixon's theory. Furthermore, it shows that we cannot include any extra term to account for the energy of the bond, which would satisfy the conservation laws. We have already seen that in this model, the total mechanical energy is not conserved in the Schwarzschild case. The only possibility for the particles to perform the prescribed motion is that there is an outer force changing their four-momentum. The description based on controlled Lagrangians is not an acceptable relativistic model.

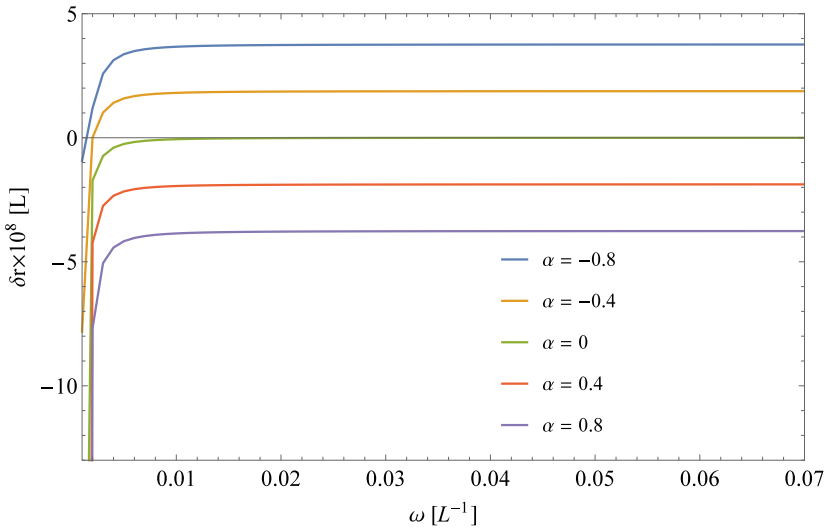

Figure 2.1: Position shifts for the glider in the de Sitter spacetime. The shifts are positive for negative values of the asymmetry parameter α. This is because the free body moves towards the cosmological horizon. This net displacement directly contradicts the results of Dixon's theory.

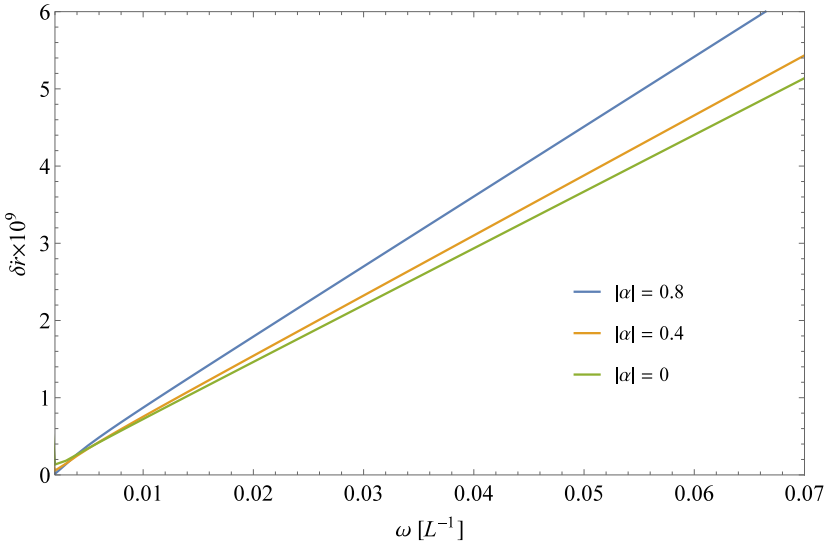

Figure 2.2: Differential velocity for the glider in the de Sitter spacetime. We can see that the differential velocity is positive in this case. The velocity shifts should also vanish according to Dixon's theory.

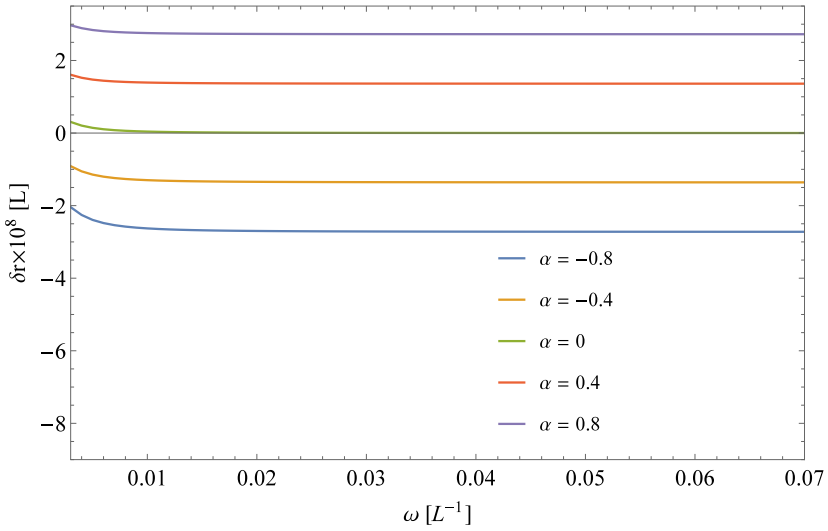

Figure 2.3: Position shifts for the glider in the anti-de Sitter spacetime. There is no divergence of the position shifts because there are no horizons in the spacetime. We had to disregard the results for the smallest values of the parameter ω because the test objects reach $r = 0$ in a finite time.

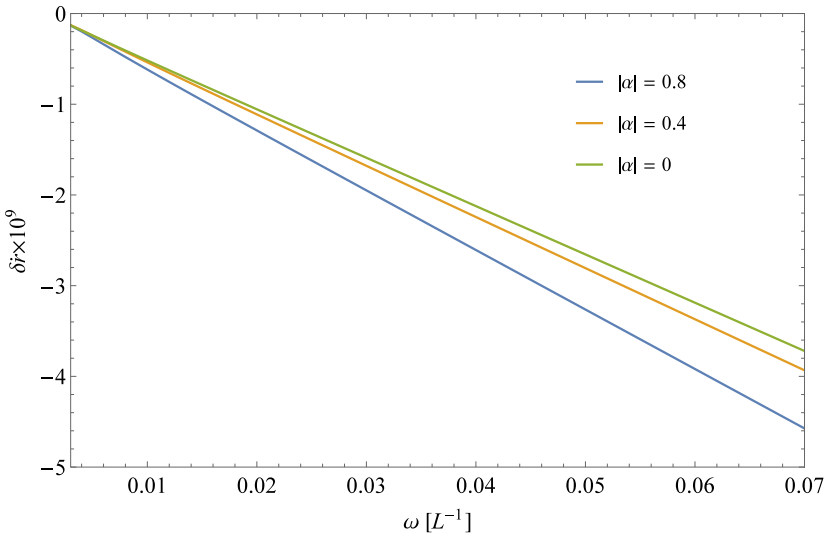

Figure 2.4: Differential velocity for the glider in the anti-de Sitter spacetime.

3. Discrete spring model of an extended body

Predictions of the glider model are in conflict with the results of Dixon's theory. The description requires non-local interaction between the endpoints of the body, which then leads to problems with causality and energy conservation. Ultimately, one has to question the validity of all predictions of the model. Can the swimming effect of the glider be reproduced using a more physically acceptable model?

In this chapter, we shall study a model of an oscillating extended body which interacts only locally and which can be described by a conserved stress-energy tensor. The system consists of several test particles which decay, collide and recombine. Each particle moves along a geodesic unless it goes through one of these processes.

Such systems have been studied in [19], where the author also shows how the momenta of such a system satisfy the equations of Dixon's theory. To achieve an attracting interaction between the particles, one has to introduce intermediate particles with negative rest masses. These negative masses can be understood as a discrete tension moving through the bond between the particles with positive masses.

Our aim is to use this model to describe a body performing motion similar to the glider and to compare the predictions of the two models regarding the final position shift. This means that we have to once again compare the final position of the body to that of a single free test particle with the same initial conditions. To avoid any problems with the definition of the centre of mass of the system, the whole process has to start with a single particle and end when all of the involved particles recombine to form a single particle again.

To evaluate the position shift we have to once again subtract values of the position of the system and the reference particle, which are very close. From the previous chapter we know that the system of colliding and decaying particles which follow a geodesic can be described by a conserved stress-energy tensor. For this model we can thus use the predictions of Dixon's theory. By studying the behaviour of the model in maximally symmetric spacetimes, where the effect must vanish, we can check its consistency and evaluate the error of the obtained results introduced by the numerical methods and representations of numbers.

In this chapter, we shall first derive the necessary equations of motion, i.e., the geodesic equations, in the chosen spacetimes (Schwarzschild, de Sitter and anti-de Sitter) using proper time and coordinate time as the independent parameter of motion. We shall also prove that the geodesic equation parametrized by the coordinate time can be derived from the action. We discuss the kinematics of decay and recombination of particle pairs. Finally, we shall find the predictions of the position shift for the discrete spring model in the three chosen spacetimes

and compare them to the glider model.

3.1 Radial geodesics in the Schwarzschild spacetime

All the particles always follow geodesic motion in the proposed model. It is thus useful to derive an explicit form of the radial geodesic equation, which we shall later solve numerically.

The model starts with a single particle with a specific initial position and velocity, decaying into a pair of identical particles moving in opposite directions. The first pair of particles moves freely until they decay, too. In the model, the decay occurs after the particle lives for a specific proper time τ_0. For this part of the process we shall, therefore, use the proper time of each particle as the independent parameter. We start from the usual form of the geodesic equation:

$$\frac{\mathrm{d}^2 x^\mu}{\mathrm{d}\tau^2} + \Gamma^\mu{}_{\alpha\beta} \frac{\mathrm{d}x^\alpha}{\mathrm{d}\tau} \frac{\mathrm{d}x^\beta}{\mathrm{d}\tau} = 0. \tag{3.1}$$

Because we are interested in the radial fall, the only relevant coordinates are r and t of the standard Schwarzschild coordinate system. First, we evaluate the necessary Christoffel symbols:

$$\begin{aligned}
\Gamma^t{}_{tr} &= \frac{\frac{M}{r^2}}{1 - \frac{2M}{r}}, \\
\Gamma^r{}_{tt} &= \left(1 - \frac{2M}{r}\right) \frac{M}{r^2}, \\
\Gamma^r{}_{rr} &= \frac{-\frac{M}{r^2}}{1 - \frac{2M}{r}}, \\
\Gamma^t{}_{tt} &= \Gamma^t{}_{rr} = \Gamma^r{}_{rt} = 0.
\end{aligned} \tag{3.2}$$

Finally, we can write down the explicit form of the geodesic equations:

$$\frac{\mathrm{d}^2 t}{\mathrm{d}\tau^2} + \frac{\frac{2M}{r^2}}{1 - \frac{2M}{r}} \frac{\mathrm{d}t}{\mathrm{d}\tau} \frac{\mathrm{d}r}{\mathrm{d}\tau} = 0, \tag{3.3}$$

$$\frac{\mathrm{d}^2 r}{\mathrm{d}\tau^2} - \frac{\frac{M}{r^2}}{1 - \frac{2M}{r}} \left(\frac{\mathrm{d}r}{\mathrm{d}\tau}\right)^2 + \left(1 - \frac{2M}{r}\right) \frac{M}{r^2} \left(\frac{\mathrm{d}t}{\mathrm{d}\tau}\right)^2 = 0. \tag{3.4}$$

This system of ordinary differential equations can be partially integrated because there are two independent conserved quantities: energy and normalization of the four-velocity. Nevertheless, it is sufficient and often numerically more stable to use these second-order equations for our purpose.

In further stages of the process, one has to check when some of the moving particles collide. Each of the particles has a different proper time and, therefore, it is more convenient to use the coordinate time as the independent variable. To do this, we have to find the equation of the radial geodesic parametrized by the coordinate time. Let us first express:

$$\frac{\mathrm{d}^2 r}{\mathrm{d}\tau^2} = \frac{\mathrm{d}}{\mathrm{d}\tau}\left(\frac{\mathrm{d}r}{\mathrm{d}t}\frac{\mathrm{d}t}{\mathrm{d}\tau}\right) = \frac{\mathrm{d}^2 r}{\mathrm{d}t^2}\left(\frac{\mathrm{d}t}{\mathrm{d}\tau}\right)^2 + \frac{\mathrm{d}r}{\mathrm{d}t}\frac{\mathrm{d}^2 t}{\mathrm{d}\tau^2}. \tag{3.5}$$

From 3.3 we can express:

$$\frac{\mathrm{d}^2 t}{\mathrm{d}\tau^2} = \frac{-\dfrac{2M}{r^2}}{1-\dfrac{2M}{r}}\frac{\mathrm{d}r}{\mathrm{d}t}\left(\frac{\mathrm{d}t}{\mathrm{d}\tau}\right)^2. \tag{3.6}$$

Finally, substituting these two expressions into 3.4 and dividing by the common factor, we obtain:

$$\frac{\mathrm{d}^2 r}{\mathrm{d}t^2} - \frac{\dfrac{3M}{r^2}}{1-\dfrac{2M}{r}}\left(\frac{\mathrm{d}r}{\mathrm{d}t}\right)^2 + \left(1-\frac{2M}{r}\right)\frac{M}{r^2} = 0. \tag{3.7}$$

This form of the equation only works for regions where t is a valid time coordinate, i.e., above the event horizon. We know that no particle can cross the event horizon in finite coordinate time and, therefore, the equation of motion should work for an arbitrarily long time interval.

3.2 Deriving the geodesic equation from the action

The geodesic equation can be derived from the action using the variational principle:

$$S = \int \sqrt{g_{\alpha\beta}\frac{\mathrm{d}x^\alpha}{\mathrm{d}\tau}\frac{\mathrm{d}x^\beta}{\mathrm{d}\tau}}\mathrm{d}\tau. \tag{3.8}$$

We do not consider variation of the independent parameter τ. The independent parameter is often chosen as the proper time but this choice is not necessary because the action is invariant under reparametrization. If we choose a different independent variable $\lambda = \lambda(\tau)$, the action is:

$$S' = \int \sqrt{g_{\alpha\beta}\frac{\mathrm{d}x^\alpha}{\mathrm{d}\lambda}\frac{\mathrm{d}x^\beta}{\mathrm{d}\lambda}\left(\frac{\mathrm{d}\lambda}{\mathrm{d}\tau}\right)^2}\frac{\mathrm{d}\tau}{\mathrm{d}\lambda}\mathrm{d}\lambda = \int \sqrt{g_{\alpha\beta}\frac{\mathrm{d}x^\alpha}{\mathrm{d}\lambda}\frac{\mathrm{d}x^\beta}{\mathrm{d}\lambda}}\mathrm{d}\lambda. \tag{3.9}$$

However, one can still doubt whether we can use one of the coordinates as the independent variable since it is one of the sought functions. Let us check this explicitly in the case of radial geodesic motion in the Schwarzschild spacetime.

The Lagrangian for this problem is:

$$L = \sqrt{1 - \frac{2M}{r} - \frac{1}{1 - \frac{2M}{r}} \left(\frac{\mathrm{d}r}{\mathrm{d}t}\right)^2}. \tag{3.10}$$

Let us denote the derivative with respect to t by a dot. We shall now find the Euler-Lagrange equation for this Lagrangian.

$$\frac{\partial L}{\partial r} = \frac{M}{r^2} \frac{1 + \frac{\dot{r}^2}{\left(1 - \frac{2M}{r}\right)^2}}{\left(1 - \frac{2M}{r}\right)^{\frac{1}{2}} \sqrt{1 - \frac{\dot{r}^2}{\left(1 - \frac{2M}{r}\right)^2}}}. \tag{3.11}$$

$$\frac{\partial L}{\partial \dot{r}} = \frac{-\dot{r}}{\left(1 - \frac{2M}{r}\right)^{\frac{3}{2}} \sqrt{1 - \frac{\dot{r}^2}{\left(1 - \frac{2M}{r}\right)^2}}}. \tag{3.12}$$

$$\begin{aligned} \frac{\mathrm{d}}{\mathrm{d}t}\left(\frac{\partial L}{\partial \dot{r}}\right) =& \frac{-\ddot{r}}{\left(1 - \frac{2M}{r}\right)^{\frac{3}{2}} \left[1 - \frac{\dot{r}^2}{\left(1 - \frac{2M}{r}\right)^2}\right]^{\frac{3}{2}}} + \\ &+ \frac{\dot{r}^2 M}{r^2} \frac{3 - \frac{\dot{r}^2}{\left(1 - \frac{2M}{r}\right)^2}}{\left(1 - \frac{2M}{r}\right)^{\frac{5}{2}} \left[1 - \frac{\dot{r}^2}{\left(1 - \frac{2M}{r}\right)^2}\right]^{\frac{3}{2}}}. \end{aligned} \tag{3.13}$$

Putting these expressions together and multiplying by the common denominator we obtain:

$$-\ddot{r} + \frac{\frac{3M}{r^2}}{1 - \frac{2M}{r}} \dot{r}^2 - \left(1 - \frac{2M}{r}\right) \frac{M}{r^2} = 0, \tag{3.14}$$

which is Equation 3.7. Thus, we showed that the time coordinate can be used as the independent variable as long as it is not degenerate, i.e., as long as it is a monotonous function of the proper time. The equation for the radial geodesic parametrized by the coordinate time can thus be derived from the variational principle.

3.3 Radial geodesic equation in the de Sitter spacetime

As we showed in the previous chapter, an extended body cannot deviate from the geodesic motion in maximally symmetric spacetimes. It is therefore a good test for any model of an extended body and for the numerical software to try to obtain this net zero position shift in the (anti-)de Sitter spacetime.

To use the proposed model in the de Sitter spacetime, we have to find the radial geodesic equation parametrized by both the proper time and the coordinate time. The derivation is very similar to the Schwarzschild case.

$$\begin{aligned}
\Gamma^{t}{}_{tr} =& \frac{-\frac{1}{3}\Lambda r}{1-\frac{\Lambda}{3}r^2}, \\
\Gamma^{r}{}_{tt} =& -\left(1-\frac{\Lambda}{3}r^2\right)\frac{1}{3}\Lambda r, \\
\Gamma^{r}{}_{rr} =& \frac{\frac{1}{3}\Lambda r}{1-\frac{\Lambda}{3}r^2}, \\
\Gamma^{t}{}_{tt} =& \Gamma^{t}{}_{rr} = \Gamma^{r}{}_{rt} = 0.
\end{aligned} \tag{3.15}$$

The geodesic equation parametrized by the proper time is then:

$$\frac{\mathrm{d}^2 t}{\mathrm{d}\tau^2} - \frac{\frac{2}{3}\Lambda r}{1-\frac{\Lambda}{3}r^2}\frac{\mathrm{d}t}{\mathrm{d}\tau}\frac{\mathrm{d}r}{\mathrm{d}\tau} = 0, \tag{3.16}$$

$$\frac{\mathrm{d}^2 r}{\mathrm{d}\tau^2} + \frac{\frac{1}{3}\Lambda r}{1-\frac{\Lambda}{3}r^2}\left(\frac{\mathrm{d}r}{\mathrm{d}\tau}\right)^2 - \frac{1}{3}\Lambda r\left(1-\frac{\Lambda}{3}r^2\right)\left(\frac{\mathrm{d}t}{\mathrm{d}\tau}\right)^2 = 0. \tag{3.17}$$

Finally, the geodesic equation in the coordinate time is:

$$\frac{\mathrm{d}^2 r}{\mathrm{d}t^2} + \frac{\Lambda r}{1-\frac{\Lambda}{3}r^2}\left(\frac{\mathrm{d}r}{\mathrm{d}t}\right)^2 - \frac{1}{3}\Lambda r\left(1-\frac{\Lambda}{3}r^2\right) = 0. \tag{3.18}$$

In this case, the time coordinate can be used in the static region under the horizon, which is located at $r_h = \sqrt{3/\Lambda}$ in the de Sitter case. In the anti-de Sitter case (negative Λ), there are no event horizons and t can be used as the independent variable everywhere. The time coordinate no longer represents the proper time of a distant stationary observer since the spacetime is not asymptotically flat. It is, however, the proper time of an observer stationary at $r = 0$.

3.4 Kinematics of the decay and the recombination of test particles

In the proposed model, all particles follow geodesics until they decay or collide with another particle. We shall only consider simple two-body decays and fusions. In this section, we shall discuss the kinematics of these processes. Let us consider a general 1+1 spacetime with a diagonal metric such as the radial part of the Schwarzschild or the de Sitter spacetime.

Let us start with the collision and fusion of two particles of masses m_1 and m_2. The mass of the product is M. Let us denote $\mu_i = m_i/M$. The motion of the product must respect the conservation of the total four-momentum:

$$\begin{aligned} \frac{\mathrm{d}t}{\mathrm{d}\tau} =& \mu_1 \frac{\mathrm{d}t_1}{\mathrm{d}\tau_1} + \mu_2 \frac{\mathrm{d}t_2}{\mathrm{d}\tau_2}, \\ \frac{\mathrm{d}r}{\mathrm{d}\tau} =& \mu_1 \frac{\mathrm{d}r_1}{\mathrm{d}\tau_1} + \mu_2 \frac{\mathrm{d}r_2}{\mathrm{d}\tau_2}. \end{aligned} \tag{3.19}$$

Here, the coordinates without a subscript correspond to the product of the collision and the coordinates with the subscript correspond to the colliding particles, t is the timelike coordinate and r is the spacelike coordinate.

Typically, the collision is described using t as the independent variable since, this way, it is easier to check if the relevant particles meet. We can express the components of the four-velocity for any particle from the normalization:

$$\frac{\mathrm{d}t}{\mathrm{d}\tau} = \frac{1}{\sqrt{-g_{tt} - g_{rr}\left(\frac{\mathrm{d}r}{\mathrm{d}t}\right)^2}} \tag{3.20}$$

and thus

$$\frac{\mathrm{d}r}{\mathrm{d}\tau} = \frac{\mathrm{d}r}{\mathrm{d}t}\frac{\mathrm{d}t}{\mathrm{d}\tau}. \tag{3.21}$$

The last equation can then be used to find the coordinate velocity of the product as well. Even though we assumed that we know the mass of the fusion product, it is not necessary. The mass of the product can be calculated from the normalization of the four-velocity.

The decay process is similar. Once again, the total four-momentum has to be conserved according to 3.19. This time, the coordinates without any subscript correspond to the decaying particle and the ones with a subscript correspond to the decay products. The components of the four-velocity of the decaying particle are known as well as the masses and we have to calculate the four-velocities of the products.

The normalization of the four-velocity for the products will give us two additional equations. Together with 3.19 these equations can be solved to find the components of the four-velocities. For example, we can derive the following equa-

tion for the spatial component of the four-velocity:

$$-\frac{4\mu_1^2}{\mu_2^4} g_{tt} \left(\frac{\mathrm{d}t}{\mathrm{d}\tau}\right)^2 - A^2 - 2AB\frac{\mathrm{d}r_1}{\mathrm{d}\tau_1} = -\frac{4\mu_1^2}{\mu_2^4} g_{rr} \left(\frac{\mathrm{d}r_1}{\mathrm{d}\tau_1}\right)^2 \tag{3.22}$$

with

$$A = \frac{\mu_1^2 - \mu_2^2 + 1}{\mu_2^2}, \tag{3.23}$$

$$B = \frac{2\mu_1}{\mu_2^2} g_{rr} \frac{\mathrm{d}r}{\mathrm{d}\tau}. \tag{3.24}$$

This is a quadratic equation for the spatial component of the four-velocity of the first product. There are two solutions in general because for a stationary decaying particle, the product can go to the left or to the right. The temporal component of the four-velocity can then be expressed from the normalization as:

$$\frac{\mathrm{d}t_1}{\mathrm{d}\tau_1} = \sqrt{\frac{1 + g_{rr}\left(\frac{\mathrm{d}r_1}{\mathrm{d}\tau_1}\right)^2}{-g_{tt}}}. \tag{3.25}$$

Finally, we can use 3.19 to calculate the four-velocity of the second product. If necessary, one can then express the coordinate velocity of the products by inverting 3.21.

3.5 Discrete spring model in the Schwarzshild spacetime

We are now ready to test the proposed model with decaying particles in a given gravitational background. First, we shall study its behaviour in the Schwarzschild spacetime. The process consists of several parts.

In the beginning, we have a stationary particle located at the position R_0. We choose its initial position to be $R_0 = 120M$ as it was in the glider model of [14]. This particle decays into two particles of the same mass and the products move in the radial direction along a geodesic with the initial velocity given by the energy of the primary decay. The initial magnitude of the velocity (both the component of the four- and coordinate velocities) is the same for both particles, only pointing in opposite directions.

This initial velocity is, in fact, a function of the masses of the products and the decaying particle. However, we shall not calculate it in this way. Rather, we simply prescribe the initial spatial components of the four-velocity for both particles. The time component of the initial four-velocity u_0 can be calculated from 3.25.

We integrate 3.4 and 3.3 for the chosen period of the proper time for both particles τ_0. This parameter would correspond to the decay rate for the particle but we shall treat it as a free parameter. After this interval of the proper time, both

particles decay into a particle with a positive mass and an exotic particle with a negative mass. Note that this decay happens at different coordinate times for the lower and higher particles. We consider the masses of the new products or, more specifically, their ratios to the mass of the decaying particle μ_1, μ_2 to be free parameters of the model. The components of the velocity of the products are calculated using 3.22 and 3.25. This means that there are two kinds of decaying particles: the initial static particle decays into two standard identical particles. These particles then undergo the exotic decay. These conditions are necessary to achieve the oscillating motion of the body.

Since we want to invent a system mimicking the behaviour of a classical oscillating spring that can exhibit tension, we have to use particles with negative rest masses because this decay has the effect that it pulls the non-exotic particles back together. The decay involving only particles with positive rest mass would only push some of the involved particles farther apart. Our goal is to fuse the particles back into one so that we can evaluate its position shift.

After both moving particles decay, all four of the created particles follow geodesic motion. For an appropriate choice of the masses, the exotic particle moves very fast towards the other pair. We are looking for the moment when one of the exotic particles reaches the non-exotic particle from the second pair. Therefore, it is more convenient to use the coordinate time as the independent variable and integrate 3.7 for all four particles at once.

We require that the exotic particles can only interact with the classical ones and they pass through one another and move towards their non-exotic partners. When one of them reaches the target particle, they collide and recombine. This process further pulls the non-exotic particle back. The four-velocity of the product is given by the conservation of the total four-momentum again. For a short period of time, we integrate the geodesic equations for the three particles until the second exotic particle reaches its target. We calculate the recombination in a similar manner.

Finally, we let the two resulting particles, which are now moving towards each other, collide, at which point we stop the integration and evaluate the position of the product. There are in total four parameters of this process: the initial velocity of the particles u_0, the decay time τ_0 and the two masses of the products μ_1, μ_2. One could also include the initial position and velocity of the primary decaying particle among the parameters but we shall only consider one set of initial conditions for now just as we shall only consider one set of initial conditions for the reference particle. We would like to compare the results of this model to the glider model from [14] and from Chapter 1. The glider model assumes a fixed maximal length of the body δl. We can approximately fix the corresponding quantity by setting $u_0 = \delta l/2\tau_0$ since this would work in flat spacetime for low velocities. The maximal length is chosen to be $\delta l = 5 \times 10^{-3} M$ in accordance with [14].

The masses μ_1, μ_2 have to be chosen appropriately because if the negative mass of

the exotic particle isn't high enough then the decay and recombination processes won't be able to pull the particles back together and the gravitational pull of the black hole would prevail. We chose $\mu_1 = 2$ and $\mu_2 = -2/5$. By this choice, the part of the motion from the exotic decay till the final merger happens very fast in comparison to the rest of the process. This allows us to easily control the total duration of the process because it is approximately equal to τ_0.

This choice effectively restricts us to a single value of the asymmetry parameter α from the glider model [14]. However, this corresponds to the positive values of the asymmetry parameter, for which the glider model yields the most interesting predictions with the largest swimming effect, i.e., a positive shift δr.

To be able to compare our results with [14] we would like to plot the dependence of the position shift on a parameter with the dimension of frequency. The whole process takes some interval of the coordinate time Δt, which is a function of the free parameters described above. We shall denote $\omega = 1/\Delta t$ and plot the position shift as a function of this ω although the actual changing parameter is τ_0.

The calculated position shifts are presented in Figure 3.1. One can clearly see that the shifts appear even in this model. The results of Dixon's theory do not exclude this possibility. However, contrary to the predictions of the glider model, the shift is always negative and vanishes for large values of ω. Once again, we notice an apparent divergence of the shifts in the region of small ω's, while the high-frequency region seems to be divergence-free. In this case, all of the particles follow geodesic motion with sub-luminal velocities because we prescribe the value of a component of the four-velocity, which is not bounded. The total stress-energy tensor of the system is conserved in terms of the covariant derivative as shown in Chapter 2. The geometric effect as the source of the divergence described in Chapter 1 is present even in this case.

However, the set of achievable values of ω is bounded from both sides. We cannot access arbitrarily small ω because if the time of decay τ_0 is too large, the particles fall too close to the event horizon (or possibly even under it). The particles then either recombine under the horizon, which takes an infinite interval of the coordinate time, or the tidal forces then pull the particles so much apart that the decays and recombinations cannot pull them back together. On the other hand, if we choose the time decay τ_0 too small, since we fix $u_0 = \delta l/2\tau_0$, the initial component of the four-velocity is very large. This means that the time-dilation effect becomes very significant. Although it takes the particles only a short period of the proper time to decay, the process takes much longer in terms of the coordinate time. This indicates that there is a maximal value of the possible value of ω for fixed values of the other parameters. We calculated the position shifts even up to this critical upper value of the parameter ω and the position shifts always approach net 0 displacement with increasing ω unlike in the case of the glider model of [14].

We cannot run into trouble with causality and energy divergence described in Chapter 1 because the model simply prevents accessing unphysical values of the parameter ω. Since the position shift is always negative, our results contradict

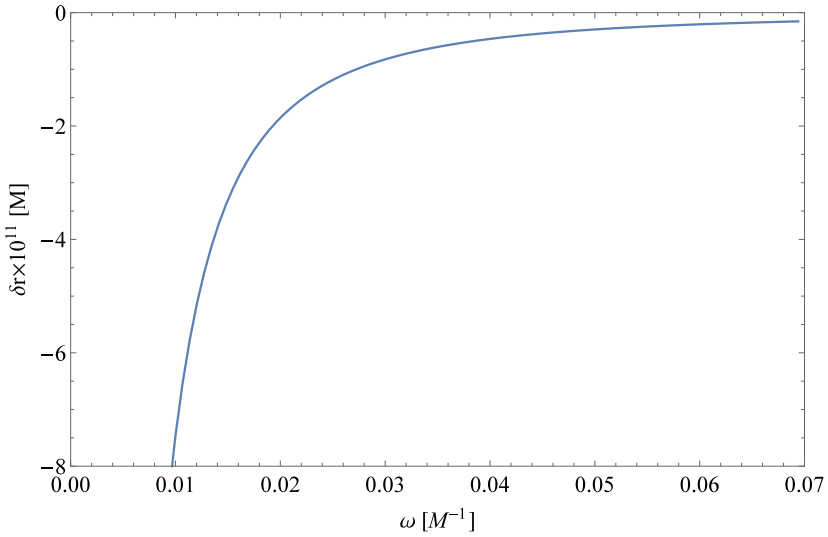

Figure 3.1: Position shifts calculated for the discrete spring model. These values were computed for the masses ratios $\mu_1 = 2$, $\mu_2 = -2/5$. Even though the particles move apart from each other for a long time and then very rapidly shrink back to a single point, which corresponds to the positive values of the asymmetry parameter from the glider model [14], the position shift is always negative and has a similar dependence on the "frequency" ω as the Newtonian glider.

the results of the glider model [14]. Moreover, the calculated position shifts are relatively smaller compared to the glider model. We effectively calculated the results only for one value of the asymmetry parameter because controlling the value of ω is rather easy in this model if we want to effectively achieve positive values of α. The situation would be significantly more complicated if we wanted to control ω while also effectively achieving the negative value of the asymmetry parameter.

Our model does not require super-luminal exchange of information among the different parts of the extended body. The predictions are thus more credible than the results of the glider model. Ultimately, the present model does not reproduce the positive values of the position shifts from the glider model in the high-frequency region for positive values of the asymmetry parameter. Therefore, we conclude that the swinging effect can only make the fall worse for the doomed swinger as they inevitably approach the horizon.

3.6 Discrete spring model in the (anti-)de Sitter universe and discussion of computational errors

In this section we shall test the model of the extended body with decaying particles in the de Sitter and anti-de Sitter spacetimes. The main purpose of this exercise is to check our numerical calculations and estimate the error of the computation. Dixon's theory predicts no net displacement of the centre of mass as

shown in the previous chapter. The reference geodesic from Dixon's theory coincides necessarily with the trajectory of a free test particle with the same initial conditions, because the body starts as a single particle.

We used Wolfram Mathematica to integrate the equations of motion and to compute the position shifts. Any calculated position shift has to be either a result of an error in the code or a numerical error. An error in the code can also result from a bias of the integration method implemented in the software.

We choose our length scale in the same way as we did in the case of the glider model [14], which means that our length unit is $L = 1/\sqrt{30000 \mid \Lambda \mid}$. In the de Sitter case, the cosmological event horizon is then located at $r_H = 300L$. The initial position of the body and the reference point particle is set arbitrarily to $R_0 = 120L$ in both cases. The reference particle starts its motion from rest and thus the two initial moving particles of the extended body have the same magnitude of the initial velocity, only with opposite directions.

The whole process goes through the same phases as it did in the Schwarzschild spacetime. In the anti-de Sitter universe we have to make sure that neither of the involved particles goes through the centre of the coordinate system $r = 0$ where the description breaks down because of the nature of the coordinate system. This means that the process must not take too much coordinate time and the particles must not move away from each other at too large velocities.

The main difference from the previous case is that we have to use the formulae derived for the case of (anti-)de Sitter case, i.e., the geodesic equations 3.16, 3.17 and 3.18. Similarly, we have to use the proper form of the kinematics formulae to calculate the relevant quantities for the decay and recombination of the involved particles. Otherwise, the calculation is very similar to the Schwarzschild case. The initial particle decays into two identical particles which move away from each other with an initial spatial component of their four-velocity u_0 for an interval of their proper time τ_0. They both decay into a standard particle and an exotic particle with mass ratios $\mu_1 = 2$, $\mu_2 = -2/5$. The exotic particles recombine with the non-exotic particle from the other pair, which pulls the particles together once again. Finally, the two remaining particles collide, at which point we evaluate the net position displacement of the whole system compared to the position of a single test particle moving along a geodesic.

Once again, the phase of the motion from the exotic decay till the end of the process takes very short time because of the choice of the mass ratios. This allows us to easily control the total duration of the process through τ_0 while keeping $u_0 = \delta l/2\tau_0$. The maximal length is set to $\delta l = 5 \times 10^{-3} L$. We present the final position shifts δr in Figures 3.2 and 3.3 as functions of $\omega = 1/\Delta t$, where Δt is the total duration of the process in terms of the coordinate time.

We computed the position shifts for the values of the parameter ω up to $1L^{-1}$. As expected, the calculated net displacement does not vanish completely in either of the two cases, which indicates the presence of numerical errors in the computa-

tion. However, the position shifts in both cases are orders of magnitude smaller than the values calculated for the body in the Schwarzschild spacetime for a given frequency ω.

To investigate the numerical errors, we then integrated the equations of motion using several different numerical methods implemented in the Wolfram Mathematica software. Two of the methods (Stiffness Switching and Extrapolation) showed a position shift comparable to that in the Schwarzschild case. These methods are likely to be biased because the net displacements are much smoother than those computed with other methods, indicating that the values are not a result of a simple rounding error. On the other hand, the methods Adams, Shooting and Explicit Runge-Kutta all show the position shift of a similar magnitude in both the de Sitter and anti-de Sitter cases. This net displacement error is many orders of magnitude smaller than the Schwarzschild case and their values appear mostly random. All three of these methods predict very similar position shifts in the Schwarzschild case.

Additionally, we computed the position shifts using different working precisions of the numerical methods. In the maximally symmetric spacetimes, the position shift always became smaller with a higher working precision. On the other hand, the values did not change very much after reaching a sufficient working precision in the Schwarzschild spacetime. Finally, we computed the net displacement for a non-vanishing initial velocity of the primary decaying particle. To calculate the initial velocities of the two decay products, one cannot simply add the initial velocity u_0. The initial components of the four-velocity have to be calculated from 3.22. We also have to compare the final position of the body to the position of a free particle with the same initial velocity. Surprisingly, the calculated net displacements were even smaller with a non-vanishing initial velocity.

All of these results show that the values computed for the case of the discrete spring model in the Schwarzschild spacetime are not heavily influenced by a numerical error. Because the model could not reproduce the positive position shifts predicted by the glider model, we have to conclude that they are the result of the unphysical characteristics of the glider model. The discrete spring model satisfying the sub-luminal interaction condition and energy-momentum conservation predicts an extended body in the Schwarzschild spacetime behaves similarly to the glider model in the Newtonian gravitational field. Moreover, the results are in agreement with the general predictions of Dixon's theory. We thus propose to use the discrete spring model to test other interesting cases, particularly a system undergoing perpendicular oscillations.

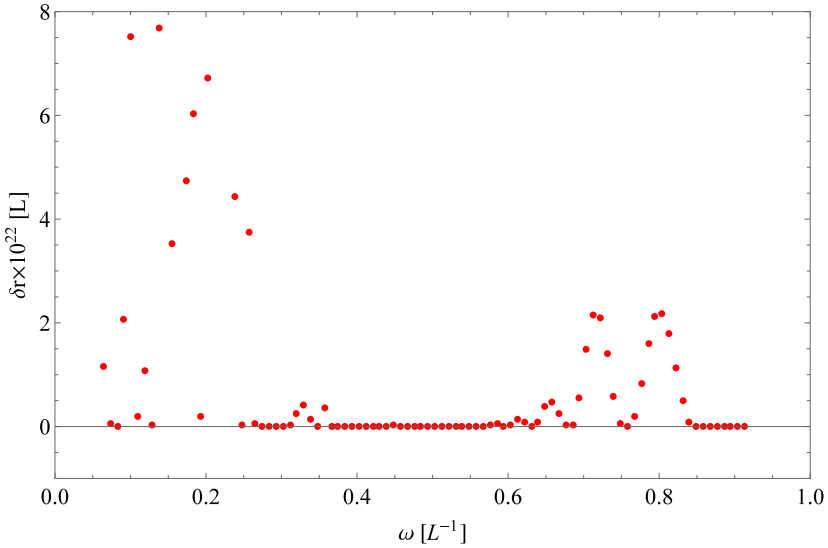

Figure 3.2: Position shifts calculated for the model with decaying particles in the de Sitter universe. These position shifts should vanish according to the results of Dixon's theory. We can see that the values are orders of magnitude smaller than those in the Schwarzschild case 3.1 and they are mostly random, which indicates the presence of a numerical error and a bias in the integration method. These values can be used as a rough estimation of the error of predictions in the Schwarzschild spacetime.

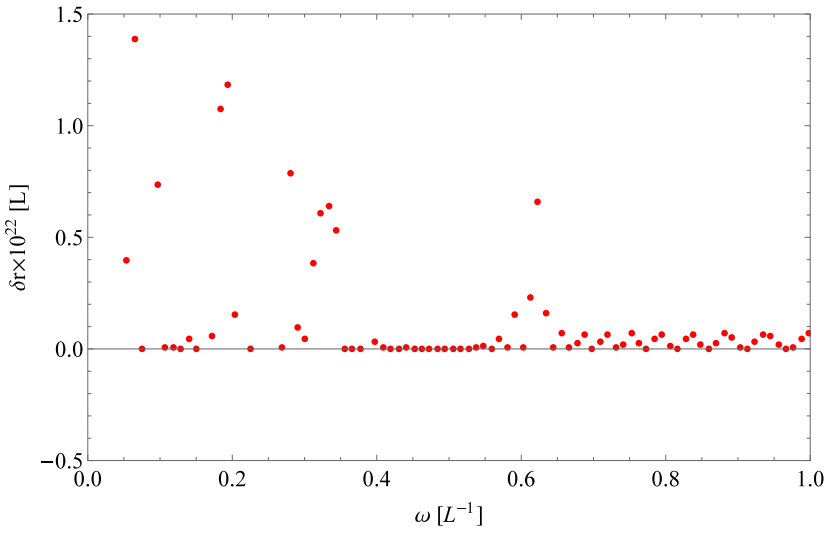

Figure 3.3: Position shifts calculated for the model with decaying particles in the anti-de Sitter universe. These values are of similar magnitude as in the de Sitter case.

Conclusions

In the first chapter of the thesis we studied the predictions of a model of an oscillating dumbbell-like body whose length was changing as a prescribed function of time. We developed a general scheme for finding the solution of equations of motion derived from a Lagrangian depending on a small scale parameter ϵ. The solution is expressed as an infinite series in terms of the small parameter. The zeroth-order solution corresponds to the solution of the equations of motion derived from the Lagrangian with $\epsilon = 0$.

The higher-order solutions are then corrections to the zeroth-order solution. We derived the equations up to the second order and also showed how the partial equations of motion for the correction can be derived directly from the Lagrangian if we express it as an infinite sum as well. We noticed that the partial equations of motion are always linear differential equations except for the zeroth-order which significantly reduces the numerics required to integrate the system in comparison to the full equations of motion.

We then applied the scheme to the glider model of an extended body. We expressed the solution of the equations of motion in terms of the maximal length of the dumbbell δl. As we expected, the zeroth-order equation is equivalent with the radial geodesic equation in the Schwarzschild spacetime. The first-order equation can also be solved analytically. In the first order, the two particles oscillate symmetrically around the trajectory of a free-falling test particle with the same initial conditions.

The second-order solution is the lowest order which predicts a deviation of the body from the geodesic motion. This explains the presence of the expression δl^2 in the semi-empirical formula for the position shifts on the plateau by the authors of the original paper about this model. We calculated the predicted position shifts by integrating the second-order partial equations for the glider in both the relativistic and the Newtonian gravitational fields. The results coincide very well with the results obtained directly by integrating the full equations of motion, which erases any doubt about the numerical credibility of the results.

We also used the approximate solution to better estimate the upper critical values of the frequency parameter ω for which one of the endpoints of the glider exceeds the speed of light and the equations of motion become singular. This estimate allowed us to carefully approach the critical values and to find a second apparent divergence of the position shift predicted by the model. We managed to compute the position shifts and differential velocities in the full interval of accessible values of the parameter ω for four chosen values of the asymmetry parameter α.

To better understand the behaviour of the glider model in the critical regimes, we studied the model of a simple dumbbell body interacting via a massless spring in the Newtonian gravitational field. The spring does not shrink back to a single point if it is falling in the gravitational field. Thus, we had to find a different

condition for evaluating the position shift. We chose the moment when the spring is maximally contracted after the first expansion. At that point, we evaluated the position shift of the geometric centre of the spring as compared to the motion of a single test particle with the same initial conditions. We saw that the dependence of the position shifts on the inverse value of the total duration of the process is similar to the predictions of the glider model in the Newtonian regime.

The spring model also revealed a problem with the description of the glider. There exists a critical value of the spring constant, which depends on the initial conditions of the body and for which the spring never stops expanding. We were able to find this critical value by the bisection method. This indicates that the bond in the glider model has to exert a diverging force on the endpoints of the glider to pull them back into a single point in the critical Newtonian region. Similarly, the rod pushes the endpoints near the speed of light in the high-frequency relativistic region. We evaluated the difference in mechanical energy before and after the maneuver. The energy input from the rod diverges in the critical regions in both the Newtonian and the relativistic model, which indicates the unphysical nature of the model.

The apparent divergence of the position shifts in the low-frequency region is much faster than in the high-frequency region. We found an explanation of this phenomenon. In addition to the troubles with the energy input from the bond, there exists a geometrical effect in the low-frequency region, which speeds up the divergence. The final position shifts are, in fact, only projections of a line on a 2-dimensional surface $\delta r = \delta r(t, \omega)$ evaluated at $t = 1/\omega$. The divergence is partially caused be the fact that we are simply integrating for longer times in the low-frequency region.

Ultimately, we had to abandon the predictions of the glider model in the critical regions because the bond would have to exert an arbitrarily large force on the body to preserve the desired deformation function of the dumbbell. This constitutes a convincing hint that the relativistic glider model is untenable and the positive shift it predicts for some values of the frequency is unphysical.

In the second chapter, we introduced the theory of extended objects in general relativity formulated by W. G. Dixon. This theory predicts the motion of any extended body described by a symmetric stress-energy tensor through a series of equations for the momenta defined for the body. For our purposes, the most important result of this formalism is that in maximally symmetric spacetimes it is possible to define the trajectory of the centre of mass of the body, which is always a geodesic if the conservation laws hold.

Furthermore, we derived the stress-energy tensor of a free test particle from the action and showed that the conservation laws for this tensor are equivalent with the geodesic equation for the particle. If we are dealing with a system of test particles, the stress-energy tensor satisfies the conservation laws if the particles only exchange energy and momentum in collisions while conserving locally the total four-momentum. The particles can also decay and recombine if the total

four-momentum is conserved.

Lastly, we used the glider model in the de Sitter and anti-de Sitter universes. Dixon's theory predicts that no net displacement of the centre of mass of the system is possible if the conservation laws hold. Since the model predicts a non-vanishing shift in both cases, we conclude that the model cannot describe a body whose individual parts only interact with one another. To achieve the prescribed motion of the body, an outer force has to act on the body. This force increases the total mechanical energy of the body. This again suggests the relativistic glider model should be replaced with a physically more plausible system.

In the third chapter, we studied a model of a test extended body consisting of several particles, where each particle moves along a geodesic until it decays or collides with another particle. We also showed that the geodesic equation parametrized by the coordinate time can be derived from the variational principle. The proposed system satisfies conservation constraints and does not require a super-luminal information transfer unlike the glider model. By involving intermediate particles with negative masses we were able to simulate an effective attractive force between the particles, achieving thus oscillating motion of the system.

Through an appropriate choice of the masses of the involved particles, we were able to achieve relative motion of the particles similar to that of the glider model described by the deformation function with a positive value of the asymmetry parameter α. By controlling the decay time of the first pair of particles, we were able to easily change the total duration of the process and then to plot the dependence of the position shift on the parameter ω corresponding to the oscillation frequency.

The obtained results show a similar dependence on the parameter ω as for the glider model in the Newtonian gravitational field. The position shift is always negative and vanishes for larger values of ω in the Schwarzschild spacetime. There exists an apparent divergence in the region of small ω's but the interval of accessible values of the parameter is bounded from below because if the particles fall too close to the event horizon or even below it, which can happen in a finite proper time, the tidal forces become too strong and the attracting process between the particles cannot pull them back together. The achievable values of the parameter ω are also bounded from above because of the time dilation effect.We conclude that there is no workable swinging effect in this case. Whatever we do, the body always ends up closer to the black hole than the reference particle.

To estimate the numerical error of the obtained position shifts, we computed the position shift of the body in the de Sitter and anti-de Sitter universes. Because the total stress-energy tensor is conserved, the position shifts have to vanish according to Dixon's theory. We changed the working precision of the methods and saw that the calculated position shifts become smaller with increasing precision in the maximally symmetric spacetimes whereas in Schwarzschild, the shift stayed almost constant after reaching a minimal necessary precision. We also used several different integration methods to compute the shifts in the (anti-)de

Sitter universe and three schemes produced values many orders of magnitude lower than the values obtained in the Schwarzschild spacetime. Furthermore, we calculated the position shifts for a non-vanishing velocity of the initial decaying particle in the maximally symmetric spacetimes. Surprisingly, the position shifts were even smaller than those calculated for a stationary initial particle.

Ultimately, we conclude that the positive position shifts obtained from the glider model are a result of the unphysical nature of its bond. We were not able to reproduce the swimming effect with our physically plausible discrete spring model satisfying conservation laws and causality conditions.

In conclusion, the goal of the thesis was to study several different models of extended bodies in general relativity and to compare their predictions. To evaluate the position shifts for the different models we came up with several analytic methods which helped us make the equations of motion more suitable for numerical integration. We added several original results concerning the energy of the proposed models as well as an explanation of the behaviour in the critical regions. We used an energy-conserving model of an extended body and showed that it agrees with the results of Dixon's theory unlike the previous glider model. In the future, we would like to study systems of extended bodies whose bond forms a continuum, such as a smooth string. The tension in the string would create an attractive interaction between the endpoints. Strings in general relativity have been studied for example in [24]. Another important and lively area of physics related to the problem of extended bodies in general relativity is the notion of self-force, i.e., the back reaction from the particle on its own motion through its gravitational, scalar or electromagnetic field. These areas deserve our close attention in the future studies.

Bibliography

[1] Misra A K a Modi V J 1986 *Advances in the Astronautical Sciences* **62** 667

[2] Souza dos Santos D P et al. 2015 *Journal of Physics: Conference Series* **641** 012004

[3] Fernández-Martínez M, López M A, and Vera J A 2016 *Nonlinear Dynamics* **84** 143

[4] Burov A A and Kosenko I I 2015 *International Journal of Non-Linear Mechanics.* **72** 1

[5] Yamagiwa Y et al. 2017 *Acta Astronautica* **138** 570

[6] Bergamin L, Delva P and Hees A 2009 *Class. Quantum Gravity* **26** 185006

[7] Andrade e Silva R, Matsas G E A and Vanzella D A T 2016 *Physical Review D.* **94** 121502

[8] Dixon W G 1970 *Proc. Roy. Soc. Lond. A* **314** 499

[9] Dixon W G 1970 *Proc. Roy. Soc. Lond. A* **319** 509

[10] Dixon W G 1974 *Philos. Trans. Roy. Soc. Lond. A* **277** 59

[11] Bloch A M, Leonard N E and Marsden J E 1997 *Proceedings CDC* **36** 2356

[12] Bezglasnyi S 2004 *Journal of Applied Mathematics and Computing* **14** 251

[13] Shiriaev A S, Freidovich L B and Spong M W 2013 *European Journal of Control* **19** 438

[14] Guéron E and Mosna R A 2007 *Physical Review D.* **75** 081501

[15] Bergamin L, Delva P and Hees A 2009 arXiv:0901.2298v3

[16] Hees A, Bergamin L and Delva P 2009 *Relativity in Fundamental Astronomy Proceedings IAU Symposium.* **261** 147

[17] Wisdom J 2003 *Science.* 2003, **299** 1865

[18] Veselý V 2017 *Motion of extended bodies in general relativity* Bachelor's thesis Charles University, Prague

[19] Slezák D 2018 *Relativistický model systému se spinem* Bachelor's thesis Charles University, Prague

[20] Veselý V and Žofka M 2019 *Class. Quantum Gravity* **36** 075011

[21] Synge J L 1960 *Relativity: the general theory.* Amsterdam: North-Holland Publ. Co.

[22] DeWitt B S and Brehme R W 1960 *Ann. Phys. (N. Y.)* **9** 220-259

[23] Helgason S 1962 *Differential geometry and symmetric spaces* New York: Academic Press.

[24] Natário J, Queimada L and Vicente R 2018 *Class. Quantum Gravity* **35** 075003

A. Appendix

IOP Publishing Classical and Quantum Gravity
Class. Quantum Grav. 36 (2019) 075011 (13pp) https://doi.org/10.1088/1361-6382/ab0976

How to glide in Schwarzschild spacetime

Vítek Veselý and Martin Žofka[1]

Institute of Theoretical Physics, Faculty of Mathematics and Physics, Charles University, V Holesovickach 2, 180 00 Prague 8, Czech Republic

E-mail: vitek.vesely@gmail.com and zofka@mbox.troja.mff.cuni.cz

Received 21 October 2018, revised 16 February 2019
Accepted for publication 22 February 2019
Published 12 March 2019

Abstract

We investigate the motion of extended test objects in the Schwarzschild spacetime, particularly the radial fall of two point masses connected by a massless rod of a length given as a fixed, periodic function of time. We argue that such a model is inappropriate in the most interesting regimes of high and low oscillation frequencies.

Keywords: geodesics, extended test bodies, harmonic oscillator, swimming in spacetime

(Some figures may appear in colour only in the online journal)

1. Introduction

We revisit the problem of a non-point-like 'glider' moving in the gravitational field of a compact object. The studied body is dumbbell-like, consisting of two massive point particles with a predetermined coordinate distance as it moves freely in a fixed gravitational field. This situation is of interest not only in the general relativistic case as a tool to distinguish various non-local effects but also in Newtonian gravity as this effect can be used to stabilize orientation of artificial satellites and even to alter their orbital parameters. In this respect, apart from the seminal thoughts of Tsiolkovsky from 1895, the first papers on tether-controlled satellites appeared in the 1960s (see [1] for a review of literature) with research continuing until this day [2–4] and there have even been in-orbit experiments (for example, the Gemini XI mission in 1966 and, more recently, STARS-C aboard ISS [5]). Likewise, in general relativity this effect can influence the trajectory of an oscillating body, pushing it into a higher or lower orbit, speeding up or slowing down its descent or ascent in a predefined background spacetime but it can also be used as a tool to investigate the properties of a given gravitational field, perhaps distinguishing between various field characteristics in the resonance regime that would remain below detection threshold with a single point particle approach. For instance, molecules oscillating near the ISCO orbit in an accretion disk near a black hole may be of interest in this respect [6].

[1] Author to whom any correspondence should be addressed.

Originally, our aim was to extend the previous general relativistic results and study the limiting cases of extremely high and extremely low glider oscillation frequencies. Ultimately, we concluded that the studied model is insufficient in the most interesting regions and should be replaced by a physically more plausible one. Paper [7] came to the same conclusion regarding a similar problem of swimming in spacetime based on a general relativistic formulation due to Dixon [8–10]. We concentrate on the simplest possible case of two point particles of equal masses, moving radially in a spherically symmetric spacetime as their distance oscillates in a predetermined manner and one is interested in whether the position of the glider after one full period is shifted with respect to a point particle moving with the same initial conditions. We use Lagrangian formulation to find the corresponding equation of motion, which we solve numerically.

For ultra-high frequencies we find an analytic approximation enabling us to see where the particles leave the null cone, rendering the model unphysical. We discuss the low-frequency region of the motion where the glider approaches the horizon and the radial shift apparently diverges. Our paper extends and generalizes previous results by covering a much wider range of frequencies, studying thus the asymptotics for both large and small frequencies, and by investigating the position as well as the velocity of the falling body. We argue that the model assuming a given form of the deformation function regardless of the resulting motion is inappropriate since it would require an infinite amount of energy to execute. To this end, starting with the Newtonian case, we propose using a harmonic oscillator with a given spring constant. We show that the shift for low frequencies is then bounded and the corresponding shift thus cannot diverge.

The paper is organized as follows: section 2 introduces the test dumbbell glider and Lagrangian formalism we use and summarizes previous results. We further explain our choice of the oscillation function. In section 3, we define the parameters of the fall that we are interested in and investigate the velocity of the dumbbell and the case of multiple oscillations. Section 4 deals with the expected asymptotic behavior of the test body for very high and very low oscillation frequencies. In the final section 5, we present a physical model of the glider in the Newtonian setting and argue against the ad hoc model. We conclude with a summary and discussion of possible generalizations and open issues.

2. The glider

The glider consists of two equal point masses that interact via a device ensuring their distance is a prescribed oscillating function of time. We can think of the device as a massless rod of a certain length, which changes with time due to an engine extending or shortening the rod. Interestingly, the whole concept is closely related to the problem of controlled Lagrangian motion used in the stabilization of satellites and underwater vehicles, for instance [11–13]. It is well defined in Newtonian physics but in GR we need to specify which length we mean. We choose here to use the coordinate length of the rod. For a given length function, approaches based on coordinate or proper length do not represent the same problem. However, for any given function it is always possible to reformulate it in terms of the other length and both represent a possible falling-body problem. Another and arguably more important aspect is whether we should be solving the problem with respect to the coordinate time t, the proper time of one of the falling bodies, or any other valid coordinate, for example the proper time of the geometric center of the body. Once again, all approaches represent different but valid problems. We will choose to state the problem with respect to the coordinate t since we cannot use a single coordinate to describe both proper times anyways. It is not obvious what this representation

would mean for observers moving with the two parts of the falling body. However, one can certainly state the final results in terms of their proper times and this description again represents a possible motion of the body.

The problem was studied in [14–16] using Schwarzschild metric of mass M and radial fall within the static region outside of the horizon. Because we choose to use the coordinate time to describe the problem, we must be especially careful when dealing with high velocities of the body. The point masses do not follow a geodesic due to the force acting between them. It is possible that at least one of the two components of the falling body would exceed the speed of light at which point the problem would no longer describe a physically acceptable motion.

To describe the motion of the dumbbell body, we adopt the Lagrangian of [14]

$$L_d = -m\sqrt{1-\frac{2M}{r_1}-\frac{\left(\frac{\mathrm{d}r_1}{\mathrm{d}t}\right)^2}{1-\frac{2M}{r_1}}} - m\sqrt{1-\frac{2M}{r_1+l}-\frac{\left(\frac{\mathrm{d}r_1}{\mathrm{d}t}+\frac{\mathrm{d}l}{\mathrm{d}t}\right)^2}{1-\frac{2M}{r_1+l}}}, \tag{1}$$

which is a sum of Lagrangians for the two point masses, which are implicitly assumed to be constant throughout the motion, and r_1 represents the radial position of the lower end of the dumbbell while l is the length of the rod, both functions of coordinate time, t. It is not obvious whether or not this Lagrangian correctly describes the problem. If the two point masses were independent, this formulation would certainly be possible and the coordinates r_1 and l would be used to derive the equations of motion. For instance, for $l \ll r_1$ we would obtain the geodesic deviation equation. However, in our case l is a given function of t. Nevertheless, we will use this approach to verify and extend the results of previous research and to identify the issues that may thus occur[2].

Preceding papers investigate a dumbbell body whose length $l = r_2 - r_1$ changes as

$$l(t) = \delta l \exp\left[\frac{(1-\alpha-2\omega t)^2}{(1+\alpha^2)\omega t(-1+\omega t)}\right], \tag{2}$$

which is a smooth function on $t \in (0, 1/\omega)$ and can be continued smoothly (as 0 or periodically, for instance) for arbitrary t. After the time $1/\omega$ the two point masses will come back together to form a single point mass and ω thus represents the frequency at which the body oscillates with respect to the coordinate time t. Here, δl is the maximal coordinate distance between the point masses and α is a dimensionless parameter, which changes the form of the oscillation curve of the body, $\alpha \in (-1, 1)$. For $\alpha = 0$ the oscillations are symmetric. For larger α, the body will expand rapidly and then contract slowly and vice versa. However, the function is not very suitable for numerical integration of the equations of motion because it is not analytic at the endpoints of the domain. Considering that the results were previously found to be independent of the precise form of the deformation function, we used the following deformation function

$$l(t) = \frac{\delta l}{2}(1 - \cos[2\pi\omega t\{\alpha(1-\omega t)+1\}]), \tag{3}$$

which is also C^1 if it is extended as 0 or periodically. We solved the equations of motion numerically with this function and verified that the effect described in literature still occurs as previously claimed. The parameter α again encodes the shape of the deformation curve.

[2] We also deal with the Newtonian case where the Lagrangian is simply the sum of kinetic and potential terms for both interacting particles. The interaction between them enters as an external force making sure the length constraint is observed at all times. We get this Lagrangian from (1) as the lowest non-constant term in the asymptotic expansion in terms of the speed of light.

3. The fall

We want to study how the body falling towards the gravitational center can change the pace of its fall by changing its length. We compare the position of the dumbbell after one oscillation with the position of a point particle—both of them falling freely from rest with the same initial radius. It has been shown that by changing the length of the body in a certain way it is possible to slow or accelerate the fall of the body as compared to the motion of a single mass. The shift is linked to an effect described by Wisdom [17] who showed how extended bodies can move actively in curved space-times by cyclic changes in shape. The equations of motion are solved numerically with initial conditions $r_1(0) = 120M, \dot{r}_1(0) = 0$. The maximal length of the body is $\delta l = 5 \times 10^{-3} M$. We denote the shift as

$$\delta r = r_1 + \frac{l}{2} - r_\mathrm{p}, \tag{4}$$

where r_p is the position of the reference particle. If evaluated at $t = 1/\omega$ when the dumbbell shrinks to a point, this quantity represents the coordinate distance between the position of the dumbbell and the position of the reference mass. For other values of t we can associate it with the coordinate distance between the geometric center of the dumbbell and the reference mass. In figure 1, we illustrate motion of the dumbbell in a Penrose diagram of the Schwarzschild spacetime.

The shifts we are interested in result from subtraction of numbers that are almost equal. Therefore, it is reasonable to ask whether the obtained results do not come from a numerical error during the integration of the equations of motion. We checked our results against previously published papers; we used both Wolfram mathematica and Maple softwares; we applied two different integration methods in Mathematica; and we developed an independent evolution scheme based on a series expansion of the difference from a reference trajectory, which we chose to be the single particle geodesic—all these results coincide where their domains overlap, with differences orders of magnitude smaller than the obtained results.

In [14] the authors present a graph that shows δr after one oscillation as a function of the frequency ω for various asymmetry parameters α. In the Newtonian case the position shift is always negative[3] and its asymptotic value for high frequencies ω is 0 for any α while in the relativistic case $\delta r > 0$ for $\alpha < 0$ and sufficiently high frequencies, which means that the dumbbell body is indeed able to slow down its fall by asymmetric oscillations, confirming the previous conclusions. Within the parameter region dealt with in [14], our results match theirs for both the Newtonian and relativistic cases. Additionally, we studied much higher and lower oscillation frequencies to investigate the asymptotic properties of the curve: paper [14] presents results for frequencies $\omega < 0.07/M$ while we managed to calculate the same quantities for frequencies up to almost $100/M$ and we present the results in section 4.

The position shifts in the Newtonian and relativistic cases are shown in figures 2 and 3, respectively. Obviously, the dependence of the position shift δr on the frequency ω in the two cases is significantly different (see also [14]): for small values of ω, the oscillating body falls very close to the event horizon where the Newtonian motion will diverge significantly from the relativistic one while for high frequencies, we approach the velocity of light. The shifts are always smaller than the distance traversed by the free-falling body within the time $1/\omega$. This means that although it is possible to slow down the fall in the relativistic case, it is not possible for the body to climb upwards in the gravitational field. In this respect it might be of interest to study an oscillating 'climber' instead, shot radially outwards from a given radius.

[3] This means that the oscillating dumbbell always falls faster than the reference mass.

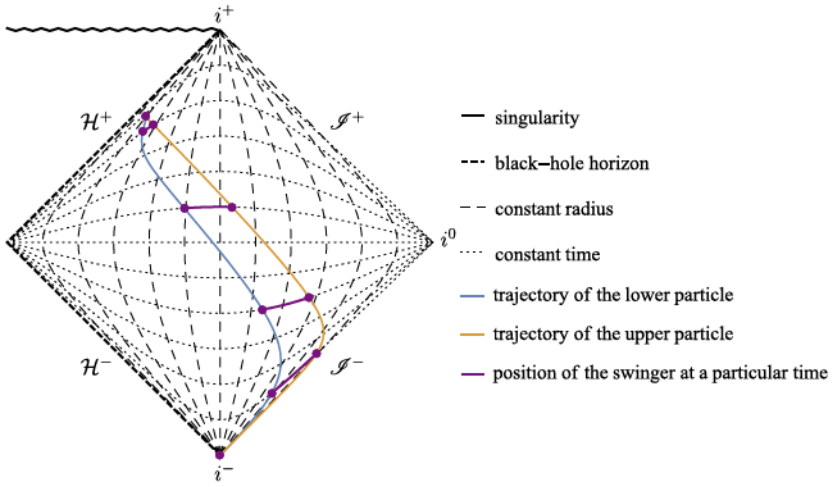

Figure 1. Penrose diagram depicting the motion of the dumbbell in a rather extreme case of $\omega = \frac{1}{107}M^{-1}$, maximal length $\delta l = 8M$, and initial distance from the center $r_1(0) = 19M$. The purple rods indicate 'snapshots' of the swinger at various fixed coordinate times throughout its oscillation cycle as it approaches the Schwarzschild radius.

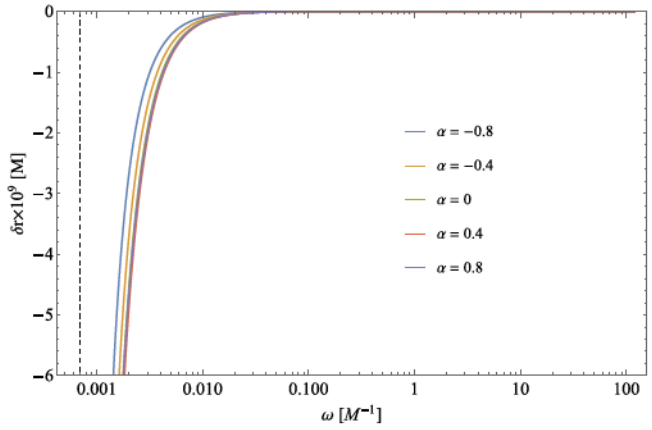

Figure 2. Newtonian shifts after one stroke are always negative and converge to 0 for large frequencies and all values of α. The dashed line represents the estimate of the smallest frequency $\omega \approx 6.8 \times 10^{-4}/M$ for which it would take the point mass time $1/\omega$ to reach the gravitational center.

Apart from the shift, we were also interested in the relative change of velocity after one or multiple oscillations since it is a crucial piece of information for subsequent evolution of the position of the body. For this purpose, we evaluated the quantity

$$\delta\dot{r} = \dot{r}_1 + \frac{\dot{l}}{2} - \dot{r}_\mathrm{p}, \tag{5}$$

which is the difference between the coordinate velocity of the geometric center of the dumbbell and the coordinate velocity of the point mass. It is of interest that $\delta\dot{r}$ is always negative

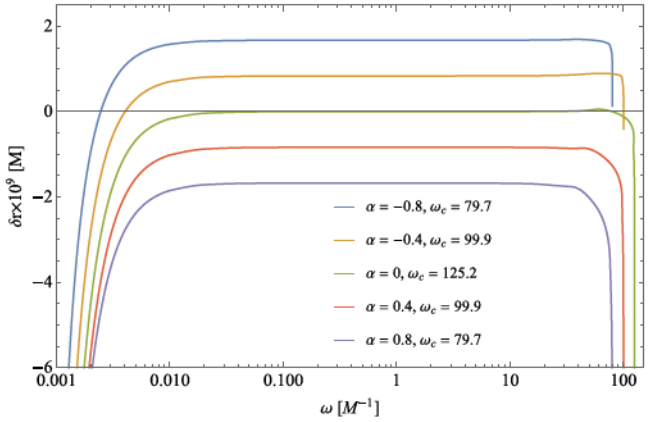

Figure 3. Relativistic shifts depend on α in a livelier manner: for $\alpha < 0$ and high enough frequencies they are positive. The curves feature a long plateau the height of which is not equal to 0 for all α's unlike in the Newtonian case and the plateau ends abruptly for $\omega_c \approx 100/M$ (the approximate critical frequencies are listed in the plot) as one of the point masses nears the speed of light, at which point the equation of motion becomes singular just like for small frequencies.

after the maneuver as can be seen in figures 4 and 5. This means that after the oscillation, the dumbbell is heading towards the gravitational center at a higher speed than the point particle. This fact may be surprising because, for $\alpha < 0$, the dumbbell falls a shorter distance than the point mass despite having a higher final velocity towards the center. That is because $\delta\dot{r}$ is mostly positive during the oscillation for $\alpha < 0$ and high enough frequencies. Thus, when integrated over time, it yields a positive difference between the position of the dumbbell and the position of the reference mass.

After completing one stroke, we can evolve the dumbbell further. We have two obvious options: either we let the dumbbell fall as a single point mass, or we let it oscillate further. In the former case, if the dumbbell has enough time before hitting the horizon, it will always end up closer to the center than the reference particle due to its higher initial speed. In the latter case however, the shift will depend on α similarly to the single oscillation case and for $\alpha < 0$ the dumbbell will fall a shorter distance than the point mass. All this of course only applies until we get too close to the horizon where our model breaks down as discussed below.

4. The fast and the slow

In figure 3 we can see that the relativistic position shift becomes highly negative for the smallest and highest values of the frequency ω and the same applies to the Newtonian case of figure 2 and low frequencies. These are the most interesting regions where the shift would be readily observable since it apparently diverges. Is that really the case? Let us first look at the upper end of the frequency spectrum in the relativistic case.

For very high oscillation frequencies it is possible that one of the point masses would exceed the speed of light, at which point the problem no longer represents a possible motion since—as confirmed by our numerical calculations—we would exert an infinite amount of work in a finite interval of time, rendering the system unphysical, see figure 6[4]. Therefore,

[4] This, in fact, applies to both the relativistic and Newtonian cases, see also figure 7.

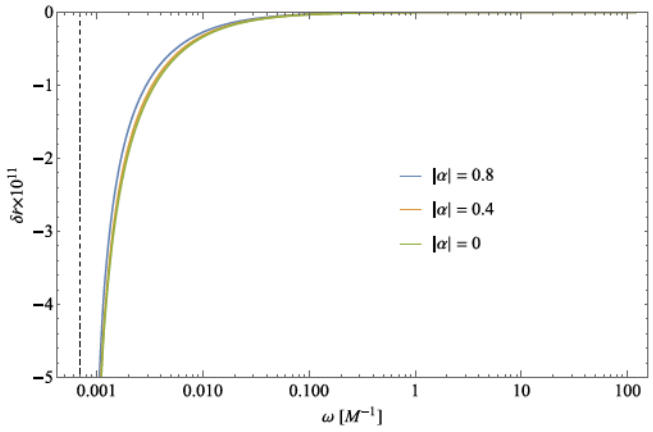

Figure 4. Differential velocity of the Newtonian dumbbell after one oscillation. The change is always negative and almost independent of the sign of α. As expected, as we approach the smallest frequencies and thus the center, $\delta\dot{r}$ diverges.

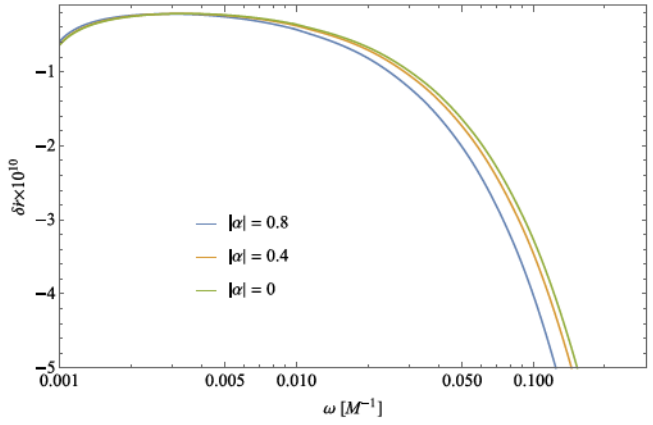

Figure 5. Surprisingly, the differential velocity of the relativistic dumbbell is also always negative despite the fact that the overall shift can be positive in some cases. This is due to the fact that the shift results from the average differential velocity while we plot here only the final value after one full oscillation. The relativistic effect is much larger than its Newtonian counterpart and diverges again for very small and very large frequencies as one of the particles hits the null cone.

the space-time interval must always lie within the null cone for both ends of the dumbbell or, alternatively, their four-velocity must be time-like. For $r_{1,2} > 2M$, the borderline condition for becoming a null trajectory reads

$$\left|\frac{\mathrm{d}r_{1,2}}{\mathrm{d}t}\right| = 1 - \frac{2M}{r_{1,2}} \tag{6}$$

for the lower and upper ends of the dumbbell, r_1 and r_2. To the first order in the expansion series with respect to the single particle trajectory, r_p, we can write $r_{1,2}(t) = r_\mathrm{p}(t) \mp l(t)/2$. For large frequencies and initial distances from the center, we can assume the center of the dumbbell is stationary, i.e. $r_\mathrm{p}(t) = R_0$. Furthermore, the deformation function (3) is of the form $l(t, \omega) = l(t\omega) = l(x)$ with $x \in [0, 1]$, yielding

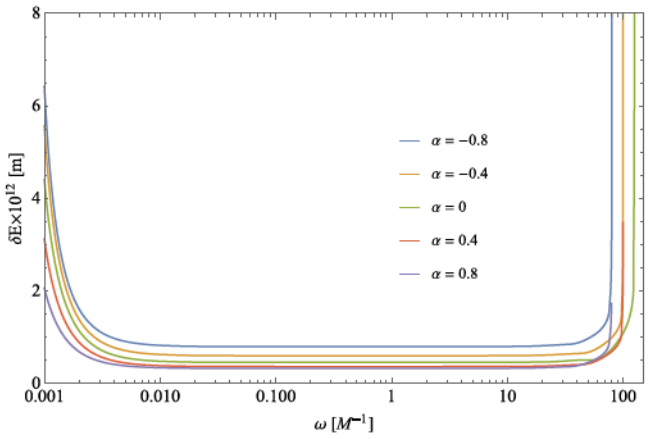

Figure 6. Total gain in energy of the relativistic dumbbell calculated as a sum of projections of the four-velocities of both particles on the timelike Killing vector. It diverges for both small and large frequencies as one of the particles approaches the speed of light. As expected, to accelerate a massive particle to such speeds requires ever more work coming from the length constraint.

$$\frac{\omega}{2}\left|\frac{\mathrm{d}l(x)}{\mathrm{d}x}\right| = 1 - \frac{2M}{(R_0 \mp \frac{l(x)}{2})}, \tag{7}$$

which we write in the form $\omega g(x) = h(x)$ providing us with a relation for ω as a function of x: $\omega = h(x)/g(x)$[5]. The sought ω is the smallest solution of this equation so that by taking a derivative and setting it equal to zero we obtain an equation for x corresponding to the extremum, $h'(x)g(x) = h(x)g'(x)$. We solve this equation numerically for the root x_0 (typically two roots and thus four roots in total for both particles) and then calculate $\omega = h(x_0)/g(x_0)$. The critical frequency is the smallest such ω.

We thus estimated the critical frequencies for all applicable values of α. The results are listed in figure 3 and coincide with the values established in our numerical integrations. They set the upper limit on the region of applicability of our model. This is the first indication that we must be careful about the Lagrangian we are using since it does not always describe the actual physics of the glider.

Let us now turn to the low-frequency section of the shift curves. In the Newtonian case the body will reach the gravitational center without completing a single oscillation if the frequency is too low. Therefore we can expect some kind of divergence for frequencies approaching a critical frequency when the body just reaches the center at time $1/\omega$ where it encounters an infinite force requiring an infinite amount of energy to maintain the prescribed length of the dumbbell, see figure 7. However, it is not obvious what kind of divergence we should expect. On the other hand, in the relativistic case the body will get closer to the event horizon at $r = 2M$. The free-falling body cannot reach the horizon in finite coordinate time t and neither can the dumbbell, which can be seen from the Penrose diagram of the space-time. We would thus expect the equations of motion to have a bounded solution for arbitrarily small values of ω. And yet, even in the relativistic case we see a divergence of the position shifts for very small frequencies. Where does it come from? There are two sources of this behavior—one is

[5] We can safely divide by $g(x) = \mathrm{d}l(x)/\mathrm{d}x$ since $g(x) = 0$ corresponds to the lowest and not the highest dumbbell expansion rate.

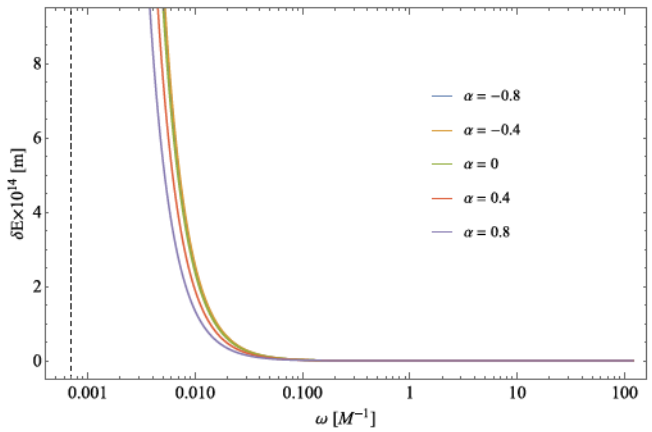

Figure 7. Total gain in energy of the Newtonian dumbbell calculated as the sum of kinetic and potential energy of both particles. As the dumbbell approaches the center, keeping the prescribed length requires ever more work to be exerted by the force ensuring the length constraint.

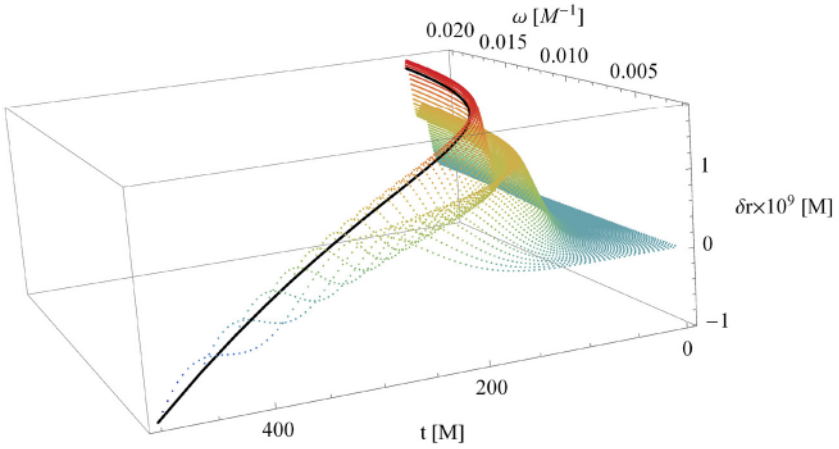

Figure 8. Shift of the geometric center of the relativistic dumbbell with respect to a single mass trajectory, as a function of time and frequency. The edge of the surface highlighted in black corresponds to one full oscillation of the spring and illustrates the origin of the apparent divergence in figure 3, see discussion below (9).

purely geometric while the other is again due to the Lagrangian we use. In figure 8, we present a 3D plot of the shift of the geometric center of the dumbbell as a function of time and frequency. This describes the dumbbell throughout its oscillation and during its entire motion while in the previous plots figures 2 and 3 we only gave its final shift for $t = 1/\omega$. In fact, we can write

$$\delta r(\omega) = \delta r(t,\omega)|_{t=\frac{1}{\omega}} = \delta r(\frac{1}{\omega},\omega) \tag{8}$$

and, for the slope of the curve, we obtain

$$\frac{\mathrm{d}}{\mathrm{d}\omega}\delta r(\omega) = \frac{\partial}{\partial\omega}\delta r(t,\omega)\bigg|_{t=\frac{1}{\omega}} - \frac{\partial}{\partial t}\delta r(t,\omega)\bigg|_{t=\frac{1}{\omega}} \frac{1}{\omega^2}. \tag{9}$$

In our numerical calculations, the partial derivatives are finite near the horizon and, therefore, we get the observed divergence. The resulting shift curve of figure 3 is included as the black cut line along the surface in the 3D figure 8 and we can see that we, in effect, run through an infinite time interval in a finite interval of ω's, producing the divergence. In fact, the same effect is at work in the Newtonian case as well.

There is, however, another cause of the divergence, which we have already discussed above for high frequencies: as we approach the horizon for small frequencies ω, one of the particles always hits the speed of light since it is pushed outside of the null cone by the requirement of a finite coordinate length of the dumbbell, which thus cannot be prescribed in this case as it would again require infinite energy, see figure 6.

The method used in [14] has also been criticised from the point of view of the covariant approach based on multipole expansions along the lines of Dixon *et al* [8–10] It is in order then to study a system that is based on a physically plausible Lagrangian and we thus chose to investigate the fall of an oscillating spring in the Newtonian setting with the same initial conditions.

5. The spring

We now use the classical Lagrangian describing two point particles of equal masses that move radially in a central gravitational field and interact via a massless spring described by a spring constant k and free length l_0 (we choose $l_0 = \delta l/2$ of (2) and (3) in order for the spring to mimic the motion of the dumbbell). The configuration of the system is given by the position of its geometric center, $X(t)$, which is also its center of mass, and its length, $l(t)$. The advantage of this approach consists in the fact that we do not need to deal with any external forces or implicitly present engines with an infinite power supply. In this case energy is obviously conserved.

$$L_s = \left(\frac{\mathrm{d}X}{\mathrm{d}t}\right)^2 + \frac{1}{4}\left(\frac{\mathrm{d}l}{\mathrm{d}t}\right)^2 + \frac{M}{X-\frac{l}{2}} + \frac{M}{X+\frac{l}{2}} - \frac{1}{2}k(l-l_0)^2. \tag{10}$$

We again drop the system from rest $X(0) = 120M, \dot{X}(0) = 0$ with zero initial distance and relative velocity of the two particles, $l(0) = 0, \dot{l}(0) = 0$. Since the spring itself is influenced by the gravitational field there is no single frequency at which the system would oscillate but we can define the period of oscillation to be the time it takes for the spring to start expanding again after the first contraction, and the frequency is then the inverse of the period. Because the dumbbell does not shrink to a point again (see figure 9), we plot the shift of its geometric center with respect to a single particle falling with the same initial conditions after the first oscillation, see figure 10. This plot is similar to figure 2 for a predefined deformation function and it confirms that in the Newtonian case the shift is always negative (the glider falls faster than a single mass) and its value is fairly independent across various deformation functions, including the spring model.

The most conspicuous feature of the plot is the apparent divergence for small frequencies, which it shares with both the Newtonian and relativistic cases of figures 2 and 3, respectively, and which is of the same geometric origin. However, since the range of admissible frequencies

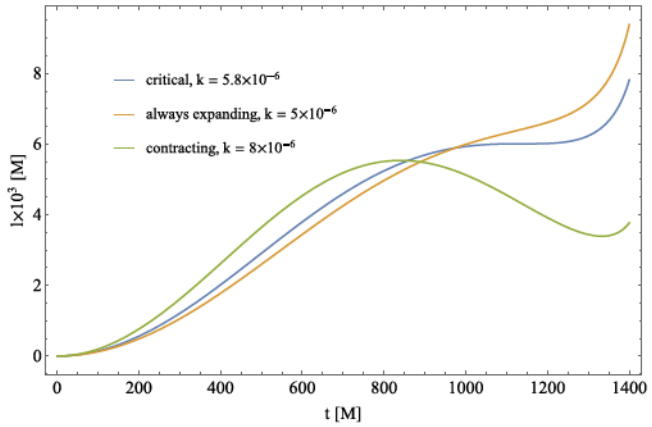

Figure 9. Evolution of the length of the Newtonian spring as a function of time for various spring constants. There is a critical spring strength, $k_c = 5.8 \times 10^{-6}/M^2$, for which the string never starts contracting again. This is due to the fact that the returning force on the lower mass grows only linearly with distance from the upper particle while the gravitational force is non-linear and, in fact, diverges close to the center.

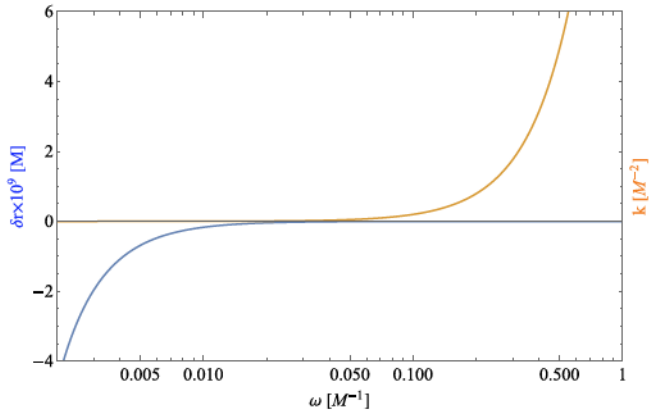

Figure 10. Shift of the geometric center of the Newtonian spring after one oscillation with respect to a single particle as a function of the effective frequency, which is a function of the spring constant. Although the shift, as a difference of two bounded values, is clearly bounded, there is again an apparent divergence for small frequencies.

is bounded it is clear there is a cutoff to the divergence and the dumbbell cannot oscillate for lower frequencies—and thus lower spring constants. The critical frequency and spring constant for our initial conditions are $\omega_c = 9 \times 10^{-4}/M$ and $k_c = 5.8 \times 10^{-6}/M^2$.

Since the energy of the system is conserved, the spring can only do a limited amount of work, which translates to the fact that a weak enough spring never starts contracting again. Requiring contraction infinitely close to the center (or to the horizon in the relativistic case) implies infinite work done by the engine shortening the dumbbell as revealed by our integrations, see figure 7. We must therefore reject the preset deformation function approach since it is unphysical in the most interesting region of low frequencies where we enter the strong gravity regions.

6. Conclusions

We studied motion of non-point masses on the background of the Schwarzschild black hole, which is closely related to the so-called swimming and swinging effects whereby an object is able to actively change its course through spacetime by altering its shape periodically. We were interested in a curious divergence observed in previous works on the subject: the relative shift of the test body with respect to a point mass starting its radial fall with the same initial conditions—this value apparently diverges for low frequencies even though, as a difference of two finite values, it must be finite. Although this feature is obviously interesting from the observational point of view, previous papers did not comment on it. We explained the low-frequency 'divergence' as a projection of a curved cross section of a 2D surface to a 1D plot combined with the fact the model is no longer tenable from the point of view of physics as one of the ends of the dumbbell touches the null cone and requires an infinite amount of energy to adhere to the prescribed deformation curve.

We further noticed an analogous divergence at the high-frequency end of the plots which is again due to the dumbbell reaching the speed of light and we found the corresponding critical frequencies. To extend our calculations and include the extreme frequency ranges, we solved the relevant equations of motion in the form of an expansion series centered on the path of a point mass. The lowest order path follows the corresponding geodesic, the first order is symmetric with respect to the geodesic, the second order yields the sought swinging effect, hence it must be proportional to δl^2. This also provides an explanation of the negative shift in the Newtonian case as the average gravitational pull on the two ends of the dumbbell is greater than the pull at the center. Additionally, we studied the relative velocity of the test body, which is always negative after a full cycle—for positive shifts, this is counterintuitive at a glance but we only look at the end of the integration interval so the overall shift can have the opposite sign[6].

The unsettling fact that the work exerted by the dumbbell engine diverges as it approaches the horizon or the center in the relativistic and Newtonian cases, respectively, together with the upper limit on admissible frequencies due to superluminal motion imply it is arguable that one should not use the implicitly troublesome model of predefined dumbbell deformation, and rather resort to some more physically explicit system such as a spring in the Newtonian case. In such a case we control the energy of the system as a whole but its specific length at each moment is also influenced by its position relative to the gravitational field. From the point of view of physics, this seems to be a more plausible approach to the problem. It is however difficult to find a general relativistic analogue of the spring since it necessarily involves non-local interaction and in our future work we intend to concentrate on precisely this topic.

Acknowledgments

VV was supported by Charles University, project GA UK 80918; MŽ acknowledges support by GA ČR 14-37086G.

ORCID iDs

Martin Žofka https://orcid.org/0000-0002-9301-8896

[6] It is perhaps of interest that a dumbbell oscillating in the azimuthal direction, perpendicular to the direction of its fall, shows relative shifts that are orders of magnitude larger than with radial oscillations. On the other hand, the results in both the Newtonian and Einsteinian cases are almost identical, rendering it rather uninteresting as a tool to study distinctly relativistic effects.

References

[1] Misra A K and Modi V J 1986 *Adv. Astronaut. Sci.* **62** 667
[2] Souza dos Santos D P *et al* 2015 *J. Phys.: Conf. Ser.* **641** 012004
[3] Fernández-Martínez M, López M A and Vera J A 2016 *Nonlinear Dyn.* **84** 143
[4] Burov A A and Kosenko I I 2015 *Int. J. Non-Linear Mech.* **72** 1
[5] Yamagiwa Y *et al* 2017 *Acta Astronaut.* **138** 570
[6] Bergamin L, Delva P and Hees A 2009 *Class. Quantum Grav.* **26** 185006
[7] Andrade e Silva R, Matsas G E A and Vanzella D A T 2016 *Phys. Rev.* D **94** 121502
[8] Dixon W G 1970 *Proc. R. Soc.* A **314** 499
[9] Dixon W G 1970 *Proc. R. Soc.* A **319** 509
[10] Dixon W G 1974 *Phil. Trans. R. Soc.* A **277** 59
[11] Bloch A M, Leonard N E and Marsden J E 1997 *Proc. CDC* **36** 2356
[12] Bezglasnyi S 2004 *J. Appl. Math. Comput.* **14** 251
[13] Shiriaev A S, Freidovich L B and Spong M W 2013 *Eur. J. Control* **19** 438
[14] Guéron E and Mosna R A 2007 *Phys. Rev.* D **75** 081501
[15] Bergamin L, Delva P and Hees A 2009 (arXiv:0901.2298v3)
[16] Hees A, Bergamin L and Delva P 2009 *Relativity in Fundamental Astronomy Proc. IAU Symp.* vol 261 p 147
[17] Wisdom J 2003 *Science* **299** 1865